

INTERSTELLAR TURBULENCE II: IMPLICATIONS AND EFFECTS

John Scalzo

*Department of Astronomy, University of Texas, Austin, Texas 78712; e-mail:
parrot@astro.as.utexas.edu*

Bruce G. Elmegreen

*IBM Research Division, Yorktown Heights, New York 10598; email:
bge@watson.ibm.com*

ABSTRACT

Interstellar turbulence has implications for the dispersal and mixing of the elements, cloud chemistry, cosmic ray scattering, and radio wave propagation through the ionized medium. This review discusses the observations and theory of these effects. Metallicity fluctuations are summarized, and the theory of turbulent transport of passive tracers is reviewed. Modeling methods, turbulent concentration of dust grains, and the turbulent washout of radial abundance gradients are discussed. Interstellar chemistry is affected by turbulent transport of various species between environments with different physical properties and by turbulent heating in shocks, vortical dissipation regions, and local regions of enhanced ambipolar diffusion. Cosmic rays are scattered and accelerated in turbulent magnetic waves and shocks, and they generate turbulence on the scale of their gyroradii. Radio wave scintillation is an important diagnostic for small scale turbulence in the ionized medium, giving information about the power spectrum and amplitude of fluctuations. The theory of diffraction and refraction is reviewed, as are the main observations and scintillation regions.

Subject headings: turbulence, elemental mixing, turbulent chemistry, cosmic rays, interstellar scintillation, interstellar medium

1. INTRODUCTION

One of the most important developments in the field of interstellar gas dynamics during the last half-century was the renewed perception that most processes and structures are strongly affected by turbulence. This is a paradigm shift unparalleled

in many other fields of astronomy, comparable perhaps to the discovery of extrasolar planets and cosmological structure at high redshift. Interstellar turbulence and its implications were commonly discussed in the 1950s, but without the range of observations that are available today, the theory of the interstellar medium (ISM) drifted toward increasingly detailed models based largely on a preference for thermal and dynamical equilibria. Standing apart were two subfields that continued to include turbulence as the primary driver of all observations: radio scintillation and cosmic ray transport. The connections between these subfields and the prevailing picture of the ISM were mostly ignored because of the large discrepancy in scales. Consequently, two other small-scale processes got lost in the equilibrium paradigm of the large-scale models: mixing of the elements and molecular chemistry. In this review, we discuss these four subfields in some detail. All have a well-established observational base going back several decades, but because of the complexity of turbulence and the infancy of the relevant theory, all of them are now in a state of rapid evolution.

Our previous review *Interstellar Turbulence I* (this volume), emphasized observations in the dense neutral ISM and discussed in detail the various theoretical approaches to this field.

2. TURBULENCE AND CHEMICAL INHOMOGENEITY

The degree to which turbulence and other transport processes mix or homogenize the gas in the face of repeated local pollutions by supernovae and other sources of fresh metals could provide an important constraint on the hydrodynamics of the ISM. This general problem is called passive scalar turbulence because the particles being transported have no effect on the velocity field. A review of experiments involving incompressible turbulent scalar transport can be found in Warhaft (2000), who emphasized that passive scalar probability density functions (pdfs) usually have strong exponential tails. A review focussing on a particular class of theoretical approaches has been given by Falkovich, Gawedzki & Vergassola (2001), whereas reviews of methods to calculate the concentration pdf and its moments are in Dopazo (1994) and O’Brien (1980). Briefer and more specialized treatments can be found in Shraiman & Siggia (2000) and Pope (2000, section 12.4).

Here we summarize observations of abundance variations in stars and gas, and we review recent theoretical work on interstellar turbulent mixing. We do not discuss star-to-star variations in globular clusters that may be affected by stellar evolution (Yong et al. 2003).

2.1. Metallicity Fluctuations: Observations

Recent observations of metallicity dispersions in stars of the same age and in interstellar gas suggest that the ISM is very well mixed on average, with typical fluctuations about the mean of only 5–20%. This low value is a challenge to explain considering the spotty pollution of new elements from supernovae and other sources. In addition, there are much larger observed fluctuations in a few places, suggesting the overall distribution function for abundance has a long, non-Gaussian tail. Both

the low dispersion and the long tail might be explained by interstellar turbulence.

Stars of a similar age have often shown large variations in metallicity (a term usually referring to iron abundance relative to the Sun). For example, Edvardsson et al. (1993) and Chen et al. (2000) found factor-of-four abundance variations in several elements for F and G main sequence stars. After correcting for selection effects, Edvardsson et al. estimated that the dispersion at a given age is about 0.15 to 0.20 dex, i.e., 40–60%, whereas Garnett & Kobulnicky (2000) suggested it is smaller than 0.15 dex for the same sample. A large unbiased sample of over 550 Hipparcos stars with homogeneous chromospheric age estimates and photometric metallicities showed a dispersion at a given age of only 0.13 dex (Rocha-Pinto et al. 2000). Reddy et al. (2003) studied 27 elements in 181 F and G stars and found a dispersion at a given age that is somewhat smaller than in Edvardsson et al. (1993) and Chen et al. (2000). Feltzing & Gonzales (2001) used an inhomogeneous sample of 5828 stars and found a larger scatter in the metallicity at a given age of 0.2 to 0.3 dex, which exceeds the observational errors. A major problem is that the ages of the stars used in these studies have large uncertainties. Considering that the stellar orbits probably migrated and led to additional abundance variations from Galactic radial gradients (e.g., Wielen et al. 1996), the stellar results are consistent with a dispersion in the gas of 20–30% or less, the upper limit set by uncertainties inherent in field star samples.

Other evidence for homogeneity among field stars comes from elemental abundance ratios. Reddy et al. (2003) estimated the intrinsic scatter in the ratio $[X/Fe]$ for element X by fitting a Gaussian curve to the histogram of deviations between $[X/Fe]$ and the linear fit of $[X/Fe]$ versus $[Fe/H]$. The standard deviations in the Gaussian for 26 elements in 181 stars varied between 0.03 and 0.10 dex. These deviations are comparable to the errors, so the result is an upper limit to the intrinsic scatter. It does not depend on stellar age, as do the absolute abundances. Reddy et al. noted that because the elements come in differing proportions from different sites of stellar nucleosynthesis, the lack of scatter implies all the ejecta were well-mixed in the gas before the stars formed.

Abundance fluctuations of 0.05–0.15 dex had also been found in studies of open clusters (e.g., Friel & Boesgaard 1992, Twarog et al. 1997, Carraro et al. 1998), B stars in star-forming regions (e.g., Cunha & Lambert 1994) and clusters (Rolleston et al. 1994), the Magellanic clouds (e.g., Olszewski et al. 1991), the interstellar medium (Meyer et al. 1998), Galactic $H II$ regions (Deharveng et al. 2000), and $H II$ regions in disk (see review in Henry & Worthey 1999) and dwarf irregular (e.g., Thuan et al. 1995) galaxies.

However, F stars in nearby open clusters (Friel & Boesgaard 1992 and references therein) show no evidence for star-to-star abundance variations at the level of detectability. Cluster-to-cluster variations are also small, including clusters of all ages, and essentially zero (less than 10–20%) for the four clusters younger than 4×10^8 years. The latter result implies that the ISM is mixed, at least to this level, for scales between ~ 1 pc (the size of the clumps from which clusters form) and ~ 100 pc (the distances between clusters) on a timescale less than 4×10^8 years. Even more stringent constraints were found from the photometric metallicity study of 76 clusters by Twarog et al. (1997). Comparison of high-precision photometry with stellar evolution models suggested a metallicity spread less than ~ 0.03 dex in the Hyades cluster (Quillen 2002). Paulson, Sneden & Cochran (2003) derived the same small $[Fe/H]$ spread, excluding three outlier stars, using spectroscopic abundance determinations

for individual stars. These results imply fluctuations of less than $\sim 7\%$ in the gas from which the Hyades cluster formed.

Interstellar absorption studies suggest equally low dispersions. Meyer et al. (1998), Moos et al. (2002), and Andre et al. (2003) found oxygen abundance dispersions over distances of around one kpc that are only a few percent. A recent study of interstellar Kr/H by Cartledge, Meyer & Lauroesch (2003) found a spread about the mean of only 0.06 dex for lines of sight within the local Orion spur; this was less than the measurement error.

We conclude that the most recent evidence, based on field stars of a given age, cluster stars, and the ISM, suggests a metallicity dispersion that is very small, less than 20 to 30% and perhaps as small as a few percent. This small Galactic dispersion is consistent with the study of 41 $H II$ regions in M101 by Kennicutt & Garnett (1996).

There are notable exceptions, though, including: (a) the existence of old super-metal-rich stars (e.g., Feltzing & Gonzalez 2001), and a large range in abundance ratios among metal-poor stars (Fields et al. 2002); (b) the lack of an age-metallicity relation for five nearby clusters, which led Boesgaard (1989) to conclude that local abundance fluctuations of ~ 0.2 – 0.3 dex must persist for at least 10^8 – 10^9 years (but see Friel & Boesgaard 1992 for a revised result); (c) the factor of 2 to 3 fluctuations in [O/H] among subgroups in Orion (Cunha & Lambert 1994), which, however, may be a result of self-pollution; (d) the study of B stars in several clusters at galactocentric distance ~ 13 kpc that indicates one cluster has [Fe/H] larger than the rest by a factor of ~ 5 (Rolleston, Dufton & Fitzsimmons 1994), (e) two stars in the Carina nebula (Andre et al. 2003) that are separated by only a few hundred parsecs but have line-of-sight oxygen abundances different by about 40%, and (f) outlier stars in the cluster studies discussed earlier.

These examples suggest a metallicity pdf with a small variance and possibly large higher moments, i.e., a fat tail at large metallicities. Such a pdf is similar to that found for the pdf of passive scalars in incompressible turbulence (Warhaft 2000). The analogous pdf for a compressible, magnetic, and self-gravitating ISM is unknown.

2.2. How Large Should Metallicity Fluctuations Be?

Theoretical investigations of abundance fluctuations have until recently nearly all been based on order of magnitude arguments involving characteristic spatial scales and timescales for various processes. Two of the more thorough discussions are in Roy & Kunth (1995) and Tenorio-Tagle (1996). Regarding spatial scales, Elmegreen (1998) pointed out that for a hierarchically structured ISM with star formation operating on a local dynamical time, the size of an O and B star association is usually larger than the supernovae remnants it produces. Unless there is some immediate mixing, as in hot ionized or evaporating flows, the new elements should be spotty and variable for subsequent generations of stars (self-enrichment). The point about timescales was highlighted by Reeves (1972): The mean time for a gas element to get reincorporated into a star is shorter than the time for its dispersal by supernova mixing, so abundance fluctuations should be large. Both results contradict the apparent uniformity of abundances inside and between clusters and in the general ISM.

Estimates for mixing times have changed since Reeves’ (1972) paper. Edmunds (1975) found that the timescale for mixing of gas by turbulence and galactic shear is relatively short compared with the star formation time, provided the sources of metals do not cluster together making the dispersion more difficult (Kaufman 1975). Bateman & Larson (1993) also derived a short mixing time, considering diffusion by cloud motions, as did Roy & Kunth (1995), who applied the diffusion approximation to galactic shear, radial flows, turbulent diffusion, supernovae, and gas instabilities. Similarly short timescales can be derived using structure functions by considering the separation of initially nearby Lagrangian fluid particles (Frisch 1995). This latter procedure is often used to derive the Richardson 4/3 law of superdiffusive incompressible turbulence. The implication of these short mixing times is that the ISM should be homogeneous.

The expectation of large spatial fluctuations may be viewed in a different way too, by considering the number of overlapping regions of contamination. Edmunds (1975) showed that n supernovae in a local volume should lead to inhomogeneities of order $n^{-1/2}$ if there is no subsequent mixing. Adopting an average of $n \sim 5 \times 10^4$, he suggested that fluctuations would be relatively small. More detailed models for overlapping contaminations were studied by Roy & Kunth (1995), Argast et al. (2000) and Oey (2000). Oey (2003) used turbulent dispersal from Bateman & Larson (1993) to enlarge the effective sizes and reduce the average metallicities in the overlapping regions. Low metallicity stars and galaxies should have large metallicity dispersions because the numbers of contaminating events are small (Audouze & Silk 1995).

A problem with most of the timescale arguments is that they apply to turbulent transport and not homogenization. Moving clouds around or shredding them with fluid instabilities does not homogenize the gas at the atomic level or change the frequency distribution of abundance concentrations; viscosity and molecular diffusion are required for that. The same is true for incompressible turbulence imagined as a cascade of vortices. Unless the advection process creates steep gradients on small scales, molecular diffusion cannot occur in a reasonable time. The situation changes when there are large-scale gradients in the mean concentration; then advection from distant regions can change the concentration distribution locally (see Equation 2 below). Even so, homogenization requires molecular diffusion. Thus, a small transport time in the ISM does not imply the gas will homogenize enough to remove abundance differences before it forms stars and clusters. The size and placement of each protostellar core within the complex spatial pattern of abundance fluctuations will determine its metallicity.

Releasing metals into the interstellar turbulent gas is similar in basic respects to dropping a blob of ink into a turbulent fluid. Figure 1 shows such a release into a two-dimensional (2D) incompressible forced chaotic velocity field (Jullien et al. 2000). Advection spreads the scalar out in space, while concentrating it locally through stretching and folding, shearing it into thin ribbons until the spatial gradients are large enough that molecular diffusion becomes significant in the third frame. By the final frame, diffusion has smeared out most of the striated structures.

How does turbulence deliver gradients to small enough scales for molecular diffusion to cause homogenization in a reasonable time? de Avezil & Mac Low (2002) found a surprisingly long timescale for the decay of the variance in a passive scalar field that had an initial checkerboard pattern and was mixed by supernovae. Their time scaled to a galaxy (at least a few times 10^8 years) is larger than previous esti-

mates and still is a lower limit because they did not include sources of new metals. de Avillez & Mac Low also found that the mixing time is independent of the mixing length, unlike mixing modeled as diffusion, and that the mixing time decreases with increasing supernova rate as a result of the increased velocities.

There may be ways other than turbulence to get gradients on small enough scales for molecular diffusion to homogenize. In Tenorio-Tagle’s (1996) “fountain with a spray” model, metal-rich droplets falling onto the disk are subject to Rayleigh-Taylor instabilities that reduce their size even further; diffusion will be very effective in such a situation.

2.3. Methods of Analysis

There are many methods for studying passive scalar turbulent transport. Here we describe two approaches: prescribed artificial velocity fields and closure methods for studying restricted properties of turbulent transport.

2.3.1. Artificial stochastic velocity fields

Most of what is known about passive scalar turbulence comes from models using an idealized velocity field that is not a rigorous solution to the hydrodynamics equations (see review by Falkovich et al. 2001). An example would be a time-uncorrelated velocity field with Gaussian statistics, a prescribed spatial correlation function, and a constraint of incompressibility. This is called a Kraichnan velocity field (e.g., Shraiman & Siggia 2000). The advantages of such a field are that the equations for the concentration field and its statistical properties can in some cases be solved analytically without a closure assumption, and the generic properties of the result might be valid for any velocity field that has the same variance and conservation constraints. However, there is a large danger in assuming a delta function for the time correlation function.

Large intermittency in the velocity gradient field means that a large fraction of the fluid contains large gradients compared with a Gaussian. In incompressible turbulence (and the ISM—see *Interstellar Turbulence I*), this fraction gets larger on smaller scales. This implies that intermittency should homogenize the gas faster than purely Gaussian motions, because molecular diffusion depends on large velocity gradients at small scales.

Decamp & Le Bourlot (2002) used another model velocity field that was obtained from a wavelet reconstruction with statistical properties similar to the ISM velocity field, including motions correlated in space and time. They solved the continuity equations and showed that the correlated velocity field has a faster dispersion and a larger standard deviation for passive scalars (by factors of 2 to 4) than an uncorrelated Gaussian velocity field. The spatial distributions for species undergoing chemical reactions were also different, suggesting a mechanism for molecular segregation in dense clouds (Section 3). Further work on turbulent mixing using synthetic velocity fields is in Elliott & Majda (1996), Fung & Vassilicos (1998), and Boffetta et al.

(1999).

2.3.2. Closure methods: PDF and moment equations

For some purposes, it may be sufficient to understand how the mean, variance, and skewness of a metallicity distribution depend on the source terms and large-scale gradients. This is the moment approach, and it has the advantage that some of its results can be obtained analytically. The moment approach might explain, for example, why there is an inverse square root scaling on the supernova rate for the decay timescale of the abundance variance (de Avillez & Mac Low 2002). The evolution equation for the one-point probability distribution of metallicities was derived rigorously for incompressible turbulence by Dopazo, Valino & Fueyo (1997), who also derived the moment equations for incompressible flow (see also O’Brien 1980; Chen & Kollman 1994; Dopazo 1994; Pope 1994, 2000).

Perhaps the simplest question that can be asked about scalar turbulence concerns the way in which the average relative concentration $\langle Z \rangle$ of a local patch of contaminant (relative to hydrogen, for example) will spread in space as a function of time. The usual place to start is to examine the mean square distance, $\langle x^2(t) \rangle$, traveled by a marked Lagrangian fluid particle. This distance can be related to an integral over the Lagrangian correlation function, assuming only statistically stationary and isotropic turbulence. Without knowing the correlation function, however, this relation is of little use. An approximation is to use the fact that the correlation is unity at time zero and approaches zero for large separations. Then for times much smaller than the correlation time $T_L = \int_0^\infty R(\tau) d\tau$, $x_{\text{rms}} = v_{\text{rms}} t$ whereas at $t \gg T_L$, $x_{\text{rms}} = 2^{1/2} v_{\text{rms}} (T_L t)^{1/2}$. Here, $R(\tau)$ is the two-time correlation function at a given point in the flow for lag τ ; i.e., $R(\tau) = \langle u(t) u(t + \tau) \rangle / \sigma^2$ for flow speed u and the average $\langle \rangle$ is over all pairs of points separated by τ . Normalization to the variance, $\sigma^2 = \langle u(t) u(t) \rangle$, makes $R(\tau)$ dimensionless with values between -1 and 1 . In this formulation, the particle behaves ballistically at short times and has an uncorrelated random walk at large times. These results are usually referred to as Taylor’s theorem (Taylor 1921; see McComb 1990; Pope 2000). The result is important for illustrating the nature of turbulence as a correlated random walk and the analogy between turbulent and molecular diffusion, where in the latter case T_L would be the mean collision time.

Klessen & Lin (2003) recently showed that Taylor’s theorem is correct in 3D-compressible turbulence. McComb (1990), Piterbarg & Ostrovskii (1997) and others have pointed out that Taylor’s theorem does not solve the problem of turbulent dispersal and transport, even for the mean field because what is required is information in the lab frame, not following the particle. Klessen & Lin (2003) suggest that the result can be used to develop a phenomenological mixing-length or diffusion model for turbulent transport in the ISM in which the integral correlation time is related to the mean time between shock passages.

Another fundamental relationship is Richardson’s law (Richardson 1926) for the rate at which pairs of points separate in space in the inertial range of turbulence. One form of this law states that the time dependence of the rms separation is $t^{3/2}$ (Falkovich et al. 2001, Boffetta & Sokolov 2002, Nicolleau & Vassilicos 2003). Work on

pair dispersion using synthetic velocity fields has resulted in at least two important insights: (a) The dynamics of particle pairs is sensitive to initial conditions but their rms separation increases algebraically, not exponentially (unlike low-dimensional chaotic systems). (b) Particle pairs travel together for long times and then separate explosively when they encounter straining regions around hyperbolic points in the flow (e.g., Nicolleau & Vassilicos 2003).

A traditional approach that could be applied to the spreading of newly produced elements from sources in the ISM is to ignore the detailed dynamics and use an equation for the evolution of the mean concentration field alone. In general, the concentration Z of an element evolves in a given velocity field \mathbf{u} as

$$\partial Z(\mathbf{x}, t) / \partial t + \mathbf{u}(\mathbf{x}, t) \cdot \nabla Z(\mathbf{x}, t) = \nabla \cdot k(\mathbf{x}, t) \nabla Z(\mathbf{x}, t) + S(\mathbf{x}, t), \quad (1)$$

where k is the mass diffusivity and S is the rate at which sources inject the element. The second term on the left represents the effect of the turbulent velocity field in advecting the concentration field. For the interstellar medium this velocity field will consist of complex compressions and vortical motions. The first term on the right represents molecular diffusion, which operates only on small scales in regions where the gradient of the concentration field is large. This equation illustrates how turbulent advection of a passive scalar spreads it out in space while increasing the local gradients through stretching, compressing, and folding. Molecular diffusion then operates where the gradients are high.

Timescales for molecular diffusion have been discussed recently by Oey (2003) for a uniform gas. The result is sensitive to temperature, so most of the homogenization of elements in the ISM may occur in the hot regions, like superbubbles (Silich et al. 2001), as well as those with the steepest velocity gradients.

To obtain the time evolution of the average concentration, one might choose to ignore all the details of the turbulence and spatially average Equation 1. Ignoring also the molecular diffusion and source terms, we get

$$\partial \langle Z \rangle / \partial t + \langle \mathbf{U} \rangle \cdot \nabla \langle Z \rangle = - \langle \mathbf{u} \cdot \nabla z \rangle = - \nabla \cdot \langle \mathbf{u} z \rangle + \langle z \nabla \cdot \mathbf{u} \rangle \quad (2)$$

for mean concentration and velocity $\langle Z \rangle$ and $\langle \mathbf{U} \rangle$ and fluctuating parts z and \mathbf{u} . The last term is zero for incompressible turbulence, leaving only $-\nabla \cdot \langle \mathbf{u} z \rangle$, which contains the unknown ensemble average of the scalar flux, $\langle \mathbf{u} z \rangle$, representing interactions between the fluctuating parts of the velocity and concentration fields. This is a classic closure problem. We could derive a differential equation for the scalar flux, but it would contain more unknown correlations, including triple correlations, and further manipulation only leads to higher and higher order unknowns.

In the incompressible case, the simplest treatment is to imagine that the turbulent transport behaves diffusively, like molecules in a gas. Then the scalar flux is proportional to the mean concentration gradient and given by

$$\langle \mathbf{u} z \rangle = -K_T \nabla \langle Z \rangle, \quad (3)$$

where K_T is a scalar diffusivity given by some timescale times the square of some velocity. Often these are taken to be the correlation time and the rms velocity, although a variety of other forms have been used to fit specific experimental results (Piterbarg & Ostrovskii 1997). Using Equation 3, Equation 2 becomes the usual

diffusion equation, and the patch of concentration, if initially a point source, would spread according to a Gaussian whose width grows $r \sim t^{1/2}$.

In fact, turbulent transport cannot be described by classical diffusion because triple correlations are as important as quadratic correlations, or, more physically, turbulent motions are not random independent steps but correlated bulk transports over a wide range of scales.

There have been many attempts, all unsuccessful to various degrees, to develop closure techniques for passive scalar turbulence. Many of these are described in reviews by O’Brien (1980) and Dopazo (1994). Perhaps the most popular in the physics community is the mapping closure suggested by Chen, Chen & Kraichnan (1989). A more complicated closure method is based on the Eddy-Damped Quasinormal Markovian approximation (Lesieur 1990). An application of this closure to the passive scalar problem with reference to earlier work is in Herr, Wang & Collins (1996).

A promising approach that is not too complex yet captures the importance of the triple correlations was proposed by Blackman & Field (2002) in connection with turbulent dynamo theory and then applied to the scalar turbulence problem (Blackman & Field 2003). The idea is to model the time derivative of the scalar flux as a normal diffusion term with an eddy viscosity plus a damping term $\langle \mathbf{u}z \rangle / \tau$, where τ is a relaxation time. This approach is similar to a closure method used in terrestrial atmospheric turbulent transport (Lewellen 1977). When this is substituted in the equation for $\langle Z \rangle$, a little manipulation results in a damped wave equation for the mean concentration. Brandenburg, Kapyla & Mohammed (2004) did extensive comparisons with numerical simulations of passive scalars in mildly compressible turbulence (rms Mach number ~ 0.2) and found good agreement with this model for the time evolution of the spreading size and the non-Gaussianity (kurtosis) of $\langle Z \rangle$.

The moment approach can derive the variance of the abundance distribution directly from Equation 1 by writing the velocity, abundance, and source fields as the sum of mean and fluctuating parts (e.g., $Z = \langle Z \rangle + z$), multiplying the resulting equation for $\partial z / \partial t$ by z , and then ensemble averaging to obtain

$$\frac{1}{2} d \langle z^2 \rangle / dt = -\frac{1}{2} \langle z\mathbf{u} \rangle \cdot \nabla \langle Z \rangle - \frac{1}{2} \langle \mathbf{U} \rangle \cdot \nabla \langle z^2 \rangle - \frac{1}{2} \langle \mathbf{u} \cdot \nabla z^2 \rangle + \langle sz \rangle + \text{diffusion}, \quad (4)$$

where s is the fluctuating part of the source term ($\langle s \rangle = 0$). The first term on the right shows how the scalar flux ($\langle z\mathbf{u} \rangle$) interacts with any large-scale gradient in the abundance, increasing variance if $\langle z\mathbf{u} \rangle$ is proportional to a mean gradient (as in Equation 3). This is analogous to how stellar orbit diffusion in the presence of a radial gradient produces fluctuations in the stellar abundances. The second term indicates that any gradient in the mean square fluctuations will be advected with the mean flow (e.g., radial flows or infall).

The third term in Equation 4 shows how turbulence can affect a concentration variance even with no gradient in $\langle Z \rangle$, zero mean velocity, and without diffusion. Writing this term as $\langle \nabla \cdot (\mathbf{u}z^2) \rangle - \langle (\nabla \cdot \mathbf{u}) z^2 \rangle$ shows that it consists of the mean divergence of the flux of scalar variance, as might be expected, minus a term that is only nonzero in the presence of compressibility. Differentiation and ensemble averaging commute, so the first term of these two is zero for a homogeneous fluid because ensemble averages do not depend on spatial position. The fourth term represents the net production of scalar variance by the fluctuating nucleosynthetic sources. “Diffusion” in this context is shorthand for the fairly complex set of second-

order derivatives involving mass diffusion at the molecular level.

As a simple illustration, assume there are no large scale flows and the abundance is linear in galactocentric distance with constant of proportionality G . For a general gradient term, we would have the triple correlation whose closure is discussed by Blackman & Field (2003) and Brandenburg, Kapyla & Mohammed (2004). Then we can also derive an equation for the correlation $\langle z\mathbf{u} \rangle$ by multiplying Equation 1 by \mathbf{u} and ensemble averaging. The result is, for $\langle \mathbf{U} \rangle = 0$,

$$\partial \langle zu_i \rangle / \partial t = - \langle u_i u_j \rangle G - \langle z (\partial p / \partial x_i) / \rho \rangle + \langle su_i \rangle + \text{diffusion}. \quad (5)$$

The first term on the right, which is $\langle u^2 \rangle G$ for an isotropic velocity field, represents the production of correlations by interaction of the velocity fluctuations with the mean metallicity gradient. We can assume that we are given some steady-state isotropic turbulent velocity field so that $\langle u^2 \rangle$ is constant. The second term on the right, often called pressure scrambling, is a serious closure problem for compressible turbulence. The source term is important if the metals come from young stars whose formation is associated with the turbulence itself, but for Type I supernovae or any other source that has time to decorrelate from the flow, $\langle s\mathbf{u} \rangle = 0$. This indicates the importance of using a consistent model for the formation of metal-producers from the turbulent field. Equations 4 and 5 can now be solved to give the evolution of the standard deviation of the abundance distribution for a particular velocity and source field.

If we neglect pressure scrambling in Equation 5 and the compressibility term in Equation 4, and also replace the triple correlation term with a simple gradient-diffusion closure, then the result would show that the concentration fluctuation variance increases $\propto \langle u^2 \rangle G^2 t^2$, even in the absence of sources. The turbulence is transporting high- z gas into low- z gas (and vice versa) due to the existence of the gradient. Obviously, after some time the large fluctuations imply steep gradients at very small scales, and so the microscopic diffusion term will cause the variance to level off. In addition, the gradient itself will be washed out by the turbulence unless there is some mechanism continually producing it. Without a sustained mean gradient, such equations could be used to understand how the variance in elemental fluctuations should decrease with time under the action of only advection and diffusion, giving a simplified model to understand the numerical decay results of de Avezil & Mac Low (2002). With some assumed closure for the source terms, or with prescribed velocity field statistics, the solution of Equation 4 would show how the abundance variance depends on the source rate.

2.4. How Do The Metals Enter the Flow?

The source terms in the transport equations depend on how the metals in expanding supernovae and superbubbles are released into the turbulent background. This is not a trivial problem, as discussed by Tenorio-Tagle (1996). Simulations of superbubbles (Korpi et al. 1999) and supernova remnants (Balsara et al. 2001) expanding into a turbulent ISM may provide guidance. Some metal-producing outflows should be jet-like, leading to the release of metals by shear flow along the walls of a chimney. Begelman & Fabian (1990) and Slavin, Shull & Begelman (1993) proposed that such turbulent layers could mix hot and warm gas, but they could just as well mix freshly-produced metals. Tenorio-Tagle (1996) suggested that superbubbles blow

out of the disk and rain down metal rich droplets that break apart by Rayleigh-Taylor instabilities. This process could disperse metals over several kpc in the disk with no assistance from disk turbulence.

These processes are also relevant for the redistribution of elements ejected by galactic blowout into the intergalactic medium (IGM). Several papers (e.g., Ferrara et al. 2000, Aguirre et al. 2001 and references therein) have noticed that it is difficult to mix metals on scales comparable to the mean distance between galaxies, requiring an additional (unknown) mechanism. Turbulence in the IGM could provide such a mechanism.

2.5. Turbulent Concentration of Dust Grains

The advection of the grains by turbulent gas can lead to spatial clustering relative to the gas, and to a spatially inhomogeneous dust-to-gas ratio. The degree of segregation depends on the grain size. Local variations in grain-grain velocities affect grain growth and shattering. Early estimates for the efficiency of this process were given by Cameron (1973), Burke & Silk (1976), Scalo (1977), and Draine (1985), but the conception of how grain advection occurs differs greatly in these papers. More rigorous derivations, aimed at grain collisions in protostellar disks but also applicable to the ISM, were given by Völk et al. (1980) and Markiewicz, Mizuno & Völk (1991).

Recent work has been directed toward trapping grains in protoplanetary disks by anticyclonic vortices (e.g., Bracco et al. 1999), which can persist for many turnover times. Large grain concentrations can result, accelerating the formation of planetesimals. Grains might also become trapped in the general ISM because of drag forces, as proposed by Falgarone & Puget (1995).

A review of experiments and simulations on turbulent gas-grain segregation was presented by Fessler, Kulick & Eaton (1994). More recent theoretical investigations (e.g., Sigurgeirsson & Stuart 2002, Lopez & Puglisi 2003) have demonstrated several interesting properties of this clustering. All of this work relies on synthetic velocity fields because inertial particle advection in real turbulent flows would require resolution much finer than the dissipation scale.

Nevertheless, the essential physics of particle drag is becoming more clear. The particle motion is dissipative even if the advecting flow is incompressible, and hence, dissipationless (Balkovsky, Falkovich & Fouxon 2001). This leads to simplified treatments in which the Stokes drag effect is modeled as a small compressible component to the velocity field of the inertial particles. A detailed study of inertial particle dynamics in incompressible flows (Bec et al. 2003) shows that particles smaller than a critical size form fractal clusters whereas larger sizes fill space with a nonuniform density. An extension to highly compressible flows is desirable.

The motion of charged dust grains in anisotropic magnetohydrodynamic (MHD) turbulence was considered by Yan & Lazarian (2002), who made a distinction between the directions parallel and perpendicular to the field. Grains with a gyration time around the field that is shorter than the gas drag time will follow the turbulent field fluctuations in the perpendicular direction. Yan & Lazarian (2003b) calculated the acceleration of charged grains that resonate with MHD fluctuations.

2.6. Turbulent Washout of Radial Abundance Gradients

Another reason to study stirring by interstellar turbulence is to understand the origin of galactic radial abundance gradients (Carraro et al. 1998, Hou et al. 2000, Rolleston et al. 2000). Models typically account for these gradients using a radially dependent timescale for infall and star formation (e.g., Chiappini et al. 2001). A problem is that turbulence should reduce large-scale gradients, so studies of this turbulent washout could give an estimate of the timescale on which the gradient must be replenished. Order of magnitude estimates along the lines of those mentioned in Section 2.2 indicate replenishment timescales larger than characteristic infall times, suggesting that contributions from a radially dependent stellar initial mass function (IMF) or other effects are not required.

A peculiar abundance gradient has been observed in the outer Galaxy, where clusters (Twarog et al. 1997) and Cepheids (Caputo et al. 2001, Andrievsky et al. 2002, Luck et al. 2003) suggest a sudden decrease in metal abundance by about 0.2 dex setting in at 10 kpc. This discontinuity appears over a radial distance less than 1 kpc. It is hard to see how such a feature could survive turbulent washout for more than 10^8 years using timescale arguments of the type summarized earlier. Either we are missing something fundamental about turbulent transport (e.g., maybe differential rotation or magnetism suppress turbulent motions in the radial direction), or this metallicity near-discontinuity does not really exist.

3. EFFECTS OF TURBULENCE ON INTERSTELLAR CHEMISTRY

The coupling of interstellar chemistry to the dynamics of interstellar gas has focused for a long time on collapsing or slowly contracting clouds (e.g., Gerola & Glassgold 1978; Prasad, Heere & Tarafdar 1991; Shematovich et al. 2003) and single shocks or MHD waves (e.g., Hollenbach & McKee 1979, 1989; Draine & Katz 1986; Charnley 1998; Flower & Pineau des Forêts 1998). The collapse models explained why early-time solutions for static chemistry often agreed better with observations than late-time solutions (e.g., Prasad et al. 1991; Nejad & Wagenblast 1999; but see Turner et al. 2000). The result that nondynamical time-dependent abundances agreed with observations for different ages is a strong motivation for the influence of turbulence because turbulent timescales are often smaller than the chemical equilibrium times. Turbulent transport can prevent the chemistry from attaining a steady state (e.g., Phillips & Huggins 1981; Xie, Allen & Langer 1995; Willacy, Langer & Allen 2002).

Turbulence can affect ISM chemistry in three ways: (*a*) by continually transporting material between regions with different physical conditions, like ambient ultraviolet (UV) radiation flux, temperature, and density, (*b*) by creating localized heating where temperature-sensitive reactions, especially those involving endothermic reactions, will be enhanced, and (*c*) by magnetically forcing ions to move faster than the thermal speed where they can enhance the temperature-sensitive ion-neutral reactions. Progress in this field is difficult because of limitations in the dynamical models and because of the large number of nondynamical chemical effects that may occur, like neutral-neutral reactions at low temperature, variable C and O depletion, three-body channels for dissociative recombination, the presence of cosmic-ray-induced UV photons, chemical phase transitions, and many more, as reviewed by Herbst (1999),

Hollenbach & Tielens (1999), van Dishoeck & Hogerheijde (1999), and Langer et al. (2000). For more recent work on chemistry covering a variety of applications not necessarily related to turbulence, see Roberts & Herbst (2002), Doty et al. (2002), Stantcheva & Herbst (2003), Shematovich et al. (2003), and Charnley & Markwick (2003).

3.1. Turbulent Transport of Chemical Species

The classic observation that implied turbulent transport was the large amount of carbon in the gas phase of dense molecular cores, considering the short freeze-out time on dust. Boland & deJong (1982) proposed that turbulent circulation could explain this discrepancy by bringing grains to the outer layers for UV desorption. Modern observations (Kramer et al. 1999) show more depletion, however, and photodissociation region (PDR) models suggest carbon comes from clump surfaces at a range of depths (Howe et al. 2000).

Turbulent transport has other applications in modern chemical models. Pijpers (1997) considered a diffusive model of turbulent grain transport and obtained a long migration time. Ragot (1998) pointed out that turbulent transport is probably neither ballistic nor diffusive, and used a model based on Levy flights to return to the smaller timescales. This transport effect is important because the degree to which CO is released from grains into the gas can affect the rest of the chemistry (CO deactivates much chemistry by depleting the H_3^+ ion; Nejad & Wagenblast 1999).

A detailed study of turbulent transport including 87 species and 1100 reactions was given by Xie et al. (1995), who assumed that radial flux is proportional to the spatial gradient of a species and used a mixing length model for turbulent diffusion. They found that most carbon-bearing species and several other important molecules were strongly affected by turbulence. The model was extended recently by Willacy, Langer & Allen (2002), who showed how the $H\ I/\text{H}_2$ ratio could provide a sensitive signature of turbulent transport. This occurs because H_2 forms when H reacts on dust grains. The formation rate depends on the density of atomic H and the total dust cross section, whereas the destruction rate depends on the UV field. If turbulence cycles material between regions with different UV optical depths on a timescale comparable to the formation time, then H will penetrate deeper into the cloud and H_2 will be closer to the surface. Because many other simple molecules are formed from H_2 -based intermediaries (especially H_3^+), turbulent transport could control the chemistry for many species.

Timescales for reaching chemical equilibrium depend on density, temperature, and ionization fraction, and are typically 10^5 – 10^7 years (van Dishoeck & Hogerheijde 1999). For the atomic part of a photodissociation region, the longest part of the cycle $\text{C}^+ \rightarrow \text{CH}_2^+ \rightarrow \text{CO} \rightarrow \text{C} \rightarrow \text{C}^+$ is the formation time of CH_2^+ through radiative association (Tielens & Hollenbach 1985) with a timescale $\sim 10^6 n_2^{-1}$ years for $n_2 =$ particle density in units of 10^2 cm^{-3} . For turbulent transport, the fastest possible timescale is ballistic, L/v , for turbulent speed v and length L . Using the ISM scaling relations for illustration (see *Interstellar Turbulence I*), this minimum time is $10^6/n_2^{1/2}$ years. The chemical and transport timescales are comparable at 10^2 cm^{-3} , but the

transport time becomes larger than the chemical time at higher density and then turbulence would seem to have little effect. Because cosmic ray ionization drives the chemistry, and each ionized H_2 molecule eventually forms CO or some other important molecule, the chemical timescale in the cores of dense clouds is the ratio of the relative abundance of CO, $\sim 10^{-4}$, to the cosmic ray ionization rate, $\sim 4 \times 10^{-17} \text{ s}^{-1}$; this gives $\sim 10^5$ years (D.J. Hollenbach, private communication).

3.2. Turbulent Heating

Another way in which turbulence may affect chemistry is through localized heating in shocks (Flower & Pineau des Forêts 1998), vortices (Joulain et al. 1998), ambipolar diffusion (Padoan, Zweibel & Nordlund 2000), and magnetic reconnection (Lazarian & Vishniac 1999). There are many reactions that seem to require higher than normal temperatures.

For diffuse clouds, the large abundance of CH^+ and molecules like HCO^+ that can form from CH^+ , and the large abundance of OH (Gredel 1997, Lucas & Liszt 1997), all suggest that high temperature ($\sim 10^3$ K) reactions take place, as in shock fronts (Elitzur & Watson 1980, Draine & Katz 1986). However, the correlation between CH^+ and the lower-temperature molecule C_2 (Gredel 1999), and the similar radial velocities of CH^+ and CH rule out CH^+ production in single large shocks or cloud surfaces. Instead, CH^+ could be made in numerous unresolved shocks that blend on a line of sight with cooler gas at the same average velocity (Gredel, Pineau des Forêts & Federman 2002). Part of the appeal of turbulence is its great range of scales that can yield such an effect.

Temperature fluctuations of several hundred degrees could play a major role in the chemistry of many species because of the inverse temperature dependence of radiative association and the range of activation energies for collisional dissociation, neutral-neutral reactions, and some ion-molecule reactions. Neutral-neutral reactions may be important even in dark clouds (Bettens et al. 1995). Prasad & Huntress (1980) long ago pointed out the importance of temperature variations in radiative association reactions and some ion-molecule reactions. Also, in dense shielded clouds, warm regions drive most of the O, OH, and O_2 to H_2O through reactions like $\text{O} + \text{H}_2 \rightarrow \text{OH} + \text{H}$ and $\text{OH} + \text{H}_2 \rightarrow \text{H}_2\text{O} + \text{H}$ (e.g., Charnley 1998), not only enhancing the H_2O abundance, but also preventing the formation of molecules like SO_2 , which rely on the oxygen species for their formation. The CN abundance should be enhanced because its destruction by reaction with O and O_2 is suppressed; this can lead to enhanced production of HC_3N through reaction of CN with C_2H_2 .

There have been several attempts to model the effects of local turbulent heating on chemistry. Black & van Dishoeck (1991) pointed out that if turbulence extends down to the collisional mean free path, then the tail of the particle velocity distribution could be enhanced. Reaction rates are averages over the particle relative velocity distribution, so energy-dependent cross-sections could have greatly enhanced rates. Spaans (1996) noted that the distribution of velocity differences in turbulent flows at small scales has a large tail and suggested this could result in non-Maxwellian relative speeds between molecules, especially those involved with CH^+ production. This assumption is questionable because the reaction scales are the mean free paths, of order

$1\text{AU}/n_2$, and these are smaller than the viscous dissipation scale of incompressible turbulence. The validity of the fluid approximation for neutrals is also questionable at these scales (see *Interstellar Turbulence I*), although MHD turbulence in the ionic component could enhance the ion-neutral collision rate.

Another approach to the problem was presented in a series of papers by Falgarone and coworkers. Falgarone & Puget (1995), Falgarone et al. (1995), and Joulain et al. (1998) considered the diffuse cloud abundances of CH^+ and several other molecules such as OH and HCO^+ . They focused on the solenoidal part of the velocity field in which molecular viscosity on 10 AU scales produces numerous local hot spots (up to several times 10^3K). Falgarone et al. (1995) showed that the resulting chemical column densities were consistent with observations. Joulain et al. (1998) used a Burgers-vortex model for the dissipation to explain other features, such as the similarity of CH and CH^+ line centroid velocities, when the number of dissipation regions on the line of sight is large.

Decamp & Le Bourlot (2002) approximated turbulence by a stochastic 1D velocity field correlated in space and time, and solved the continuity equation for the density of each species. For a small reaction network, the abundances developed different patterns on different scales, showing how species segregation can occur in a turbulent flow. Species that do not normally peak at the same time for a non-turbulent model can coexist in a turbulent model, which means that the age of a region cannot be inferred from the abundances. The issue of chemical differentiation is important because it is well-established and unexplained in a number of starless cores such as TMC-1, L134N, and L1544, and observed as 1–10 AU variations in CO, H_2CO , and OH relative to H_2 toward extragalactic background sources (Marscher, Moore & Bania 1993; Moore & Marscher 1995; for more recent work, see Pan, Federman & Welty 2001; Rollinde et al. 2003; Stanimirovic et al. 2003). Although some of these variations may be attributed to freeze-out of molecules on dust grains (Bergin et al. 2002), most are probably also affected by time-dependent chemistry (Langer et al. 2000). One important timescale is cloud contraction (Shematovich et al. 2003), but another is turbulent cycling between different physical conditions over a range of timescales (Decamp & Le Bourlot 2002). The observed variations at scales so small that gravity is unimportant seem to favor turbulence. The calculations by Decamp & LeBourlet also develop a bistable chemical pattern in which dual equilibria are possible. However, it is not known how many of the effects result from the imposed artificial velocity field, which is not able to react to the changing density field through pressure.

The only truly hydrodynamical turbulence simulation that included a small but relevant chemical reaction subset was by Pavlovski et al. (2002), who generalized previous work by Mac Low and coworkers to include a large number of coolants and a wide range of possible temperatures and densities. The reaction network in Pavlovski et al. included H, C, O, and five molecules formed from them, and it included H_2 formation on grains. They followed the decay of hypersonic turbulence without self-gravity in a dense (10^6 cm^{-3}), small (10^{16} cm) region. Their surprising result was that after H_2 dissociated in a shock, the molecules reformed in a pattern of filaments, clumps, and diffuse gas yet the abundances were fairly uniform after only 100 years.

There are probably other processes that produce localized regions of hot chemistry. For example, ambipolar diffusion heating depends on a high-order derivative of the magnetic field and so can produce heating rates that exceed the average rate

by orders of magnitude on very small scales (Padoan, Zweibel, & Nordlund 2000). Magnetic reconnection (Lazarian & Vishniac 1999) is another possibility for localized hot gas. The chemistry induced by these processes has not yet been investigated.

4. COSMIC RAY SCATTERING AND ACCELERATION IN A TURBULENT INTERSTELLAR MEDIUM

Cosmic rays scatter off magnetic waves and MHD turbulence as the particles propagate along magnetic field lines, and they generate waves and turbulence if they stream much faster than the local Alfvén speed. Observations of cosmic rays at the Earth and of radio and X-ray emissions produced by cosmic rays at their sources and throughout the Galaxy suggest the ISM is filled with irregularities on the scale of a particle gyroradius. This ranges from 1 AU to 1 pc for protons with energies between a few GeV and the knee of the cosmic ray energy distribution at 10^{15} eV. This section reviews the connection between cosmic rays and turbulence. It is not known if the turbulence that scatters cosmic rays has the same origin as the turbulence on larger scales, i.e., whether it is part of an energy cascade from these larger scales. It could be generated locally, for example, by the cosmic rays themselves or in other small scale instabilities (see also section 3, *Interstellar Turbulence I*), and it could be more similar to scintillation turbulence, which has the same small scale (Section 5) than molecular cloud turbulence, which is presumably generated on much larger scales. Other reviews of cosmic rays are in Cesarsky (1980), Berezhinskii et al. (1990), Drury et al. (2001), Jokipii (2001), Ptuskin (2001), and Schlickeiser (2002).

The important point about cosmic rays from the perspective of this review is that they scatter frequently, diffusing rather than streaming through the Galaxy. Their total path length determined from the ratio of secondary to primary nuclei is equivalent to 10^4 Galactic disk crossings at GeV energies (Engelmann et al. 1990, Higdon & Lingenfelter 2003). Their flight time determined from isotope ratios ranges from ~ 15 My for a leaky-box model with a small halo (Simpson & Garcia-Munoz 1988, Yanasak et al. 2001) to 10^8 years for a diffusion model in a ~ 5 kpc halo (Ptuskin & Soutoul 1998). They scatter so frequently that their flux at the Earth is isotropic to within 5×10^{-4} (Cutler & Groom 1991, Munakata et al. 1997), even though there are only a handful of nearby sources (i.e., Geminga, Vela, Lupus Loop, Loop III—see Ptuskin & Soutoul 1998, Jones et al. 2001, Taillet & Maurin 2003).

The scattering distance, λ , is the step size in a random walk over the Galactic thickness H (Achterberg, Blandford & Reynolds 1994). For N random isotropic scatterings, $H = N^{1/2}\lambda$, so for total distance travelled $vt = N\lambda$ with $v \sim c$ particle speed, we get $\lambda = H^2/vt = 0.2 \text{ pc} (H/\text{kpc})^2 / (t/15 \text{ My})$ at GeV energies. This is a very small distance on galactic scales, but still much larger than a gyroradius, $R_G = \gamma\beta_r \sin\alpha mc^2 / (ZeB_0)$ for rest mass m , relativistic $\beta_r = v/c$, and $\gamma = (1 - \beta_r^2)^{-1/2}$, magnetic field strength B (Gauss) and charge Ze with $e = 4.803 \times 10^{-10}$ esu. In the expression for R_G , the angle of particle motion with respect to the field line is α . Taking $\beta_r \sim 1$ and $\sin\alpha \sim 1$, we get $R_G \sim 3.3 \times 10^{12} E_{\text{GeV}} / (ZB_{\mu\text{G}})$ cm for hadron particle energy E_{GeV} in GeV and field strength $B_{\mu\text{G}}$ in microGauss. Thus, the mean scattering distance for GeV energies is $\sim 10^5$ gyroradii and the gyroradius has the same scale as the Solar system.

The relative amplitude of the magnetic irregularities $\delta B/B_0$ that have the size R_G may be determined from the random walk of angular deflections, $\Delta\phi$, which build up in proportion to the square root of the number N_G of gyrations as $\Delta\phi \sim N_G^{1/2} \delta B/B$ for small $\delta B/B$. The scattering frequency is $\nu \equiv v/\lambda = \Delta\phi^2/t$, and the number of gyrations is $N_G = \Omega t$ for gyrofrequency $\Omega = v/R_G$. Thus, $\nu = \Omega (\delta B/B)^2$ and $\delta B/B_0 = (R_G/\lambda)^{1/2} \sim 2 \times 10^{-3}$ when $\lambda \sim 0.2$ pc. Evidently, magnetic fluctuations of less than one percent on 0.1 AU scales can isotropize cosmic rays with GeV energies; in general, a wide spectrum of fluctuations is needed to scatter the full energy range. This level of irregularity is much smaller than observed on > 10 pc scales from pulsar dispersion measures, which suggest $\delta B \sim 5\mu\text{G}$ and $\langle B \rangle \sim 1.5\mu\text{G}$ (Rand & Kulkarni 1989). It is also smaller than the integrated fluctuations found by scintillation on scales less than 3.5 pc, which give $\delta B \sim 0.9\mu\text{G}$ and $\langle B \rangle \sim 3\mu\text{G}$ (Minter & Spangler 1997), and smaller than $\delta B/B \sim 1$ from optical polarization (Heiles 1996, Fosalba et al. 2002). A spectrum of magnetic energy fluctuations like the Kolmogorov or Kraichnan spectra will make $\delta B/B$ much smaller on the scale of the gyroradius than these observed field irregularities. Such a spectrum will also give the required rigidity dependence for the diffusion coefficient (Strong & Moskalenko 1998). The rigidity of a cosmic ray is $\gamma\beta_r mc^2/Ze$.

Cosmic rays can also scatter off strong magnetic irregularities having a scale comparable to or larger than R_G (Jokipii 1987). Inverting the above expression and integrating over a spectrum of waves $\propto (k/k_{min})^{-q}$, the mean free path is $\lambda \sim (B/\delta B)^2 R_G (k_{min} R_G)^{1-q}$ (Schlickeiser 1989). For $\delta B/B \sim 1$ and a particle gyroradius that fits inside the compressed region, $R_G \leq k_{min}^{-1}$, this gives $\lambda \sim R_G$. If the scattering arises in a network of strong shocks in a supersonically turbulent medium, then the mean free path for diffusion will be about the shock separation. Because the gyroradius of GeV protons is less than the collision mean free path for atoms and ions, collisional MHD models of compressible turbulence do not apply to these small scales (see *Interstellar Turbulence I* and Section 4.2 below).

4.1. Cosmic Ray Scattering in Magnetic Waves

The field line fluctuations that scatter cosmic rays could be coherent waves, stochastic turbulence, or shock fronts. One common view of waves is that they are weak fluctuations compared with the mean field, with wave travel times much longer than an oscillation period and a well-defined dispersion relation between frequency and wavenumber. Particles in such a wave field interact successively with many crests, travelling rapidly along the field until their cumulative pitch angle deviation becomes large and they begin to interact with a different wave train. A turbulent medium is not so regular but particle interactions with a broad wave spectrum can be similar as long as the particle sees a magnetic perturbation with the right wavelength after each gyration. In both cases the field can be treated as static for the fast-moving particles.

Much of the history of cosmic ray theory is based on observations of the solar wind, which contains a mixture of weak and strong fluctuations, depending on frequency (Dröge 1994; Goldstein, Roberts & Matthaeus 1995). Perhaps $\sim 15\%$ of it is

in the form of slab-like Alfvén waves ($k_{\perp} \sim 0$) and $\sim 85\%$ is two-dimensional (2D) magnetic turbulence ($k_{\parallel} \sim 0$, Bieber, Wanner & Matthaeus 1996). Here, k_{\perp} and k_{\parallel} are wavenumbers perpendicular and parallel to the mean field. The solar wind observations led to the quasilinear theory of cosmic ray propagation (Jokipii 1966), which assumes the field is uniform in space and unchanging in time over a particle gyration. Interstellar applications of this theory may be appropriate at high spatial frequencies where weak electron perturbations scatter radio waves (Section 5), or near shock fronts where weak waves on either side scatter relativistic particles back and forth (Section 4.3), or for waves that are excited by the cosmic rays themselves (Chandran 2000a). The waves cause cosmic rays to diffuse in both momentum and space (e.g., Schlickeiser 1994). Momentum diffusion means that velocities change and isotropize; space diffusion means that cosmic rays spread out slowly to more uniform densities. The two diffusion coefficients are inversely related: Higher momentum diffusion means lower spatial diffusion as the particles isotropize their velocities more easily.

There are two types of waves that could be important for cosmic ray scattering. Alfvén waves are transverse oscillations with a restoring force from field line tension and a frequency less than the ion gyro frequency. Their dispersion relation between frequency ω and wavenumber k is $\omega^2 = v_A^2 k^2 \cos^2 \theta$ for angle θ between the wave propagation vector and the average field. Their group and phase velocity parallel to the mean field is the Alfvén speed $v_A = B / (4\pi\rho_i)^{1/2}$ for ion density ρ_i . When thermal pressure with sound speed a contributes to the restoring force there are also magnetosonic waves with the dispersion relation

$$\omega^2 = 0.5k^2 \left(a^2 + v_A^2 \pm \left[(a^2 + v_A^2)^2 - (2av_A \cos \theta)^2 \right]^{1/2} \right). \quad (6)$$

The positive and negative signs are for fast and slow waves. For oblique propagation of magnetosonic waves, when $\cos \theta \sim 0$, the phase speed of the fast mode can be large along the field lines: $v_A / \cos \theta$ in the low β limit (β is the ratio of thermal to magnetic pressures, $= 2(a/v_A)^2$) and $a / \cos \theta$ in the high β limit. This speed is important for cosmic rays because they also move quickly along the field lines and will resonate with the magnetic fluctuations in these waves. Oblique magnetosonic waves also have a magnetic pressure that varies slightly along the field as a result of the successive convergences and divergences of the velocity and field, which are in phase for fast waves and out of phase for slow waves. These field line changes create magnetic mirrors that enhance the scattering (Schlickeiser & Miller 1998, Ragot 2000).

The condition for resonance between a cosmic ray and a wave is (Jokipii 1966, Hall & Sturrock 1967, Hasselmann & Wibberenz 1968)

$$\omega - k_{\parallel}v_{\parallel} = n\Omega. \quad (7)$$

This expression says that the Doppler shifted frequency of the magnetic wave, as viewed by the particle moving parallel to the field at speed $v_{\parallel} = v\mu \equiv v \cos \alpha$ for pitch angle α , equals an integer number, n , of the gyration frequency. For an Alfvén wave, $\omega = k_{\parallel}v_A$, and for a fast mode at low β , $\omega = kv_A$. The case $|n| \geq 1$ is gyroresonance. For wave spectra that decrease with k as a power law, only the lowest-order resonances ($n = \pm 1$) are important (Cesarsky & Kulsrud 1973).

Magnetosonic waves have an additional resonance for $n = 0$ (Lee & Völk 1975, Fisk 1976, Achterberg 1981), when particles stay between two crests by moving along the field at the parallel wave speed. Such a particle slows down when it hits the compressive part of the wave ahead of it (by the mirror effect), and it speeds up if the compressive part hits the particle from behind. As a particle oscillates between crests, it can have a parallel velocity that resonates with another wave moving faster along the field, and then jump over to become trapped between two new crests. For a broad wave spectrum, the particle jumps from one wave to the next, gaining energy on average. This process is called transit time acceleration of particles or transit time damping (TTD) of waves (Miller 1997, Schlickeiser & Miller 1998). TTD increases the parallel component of cosmic ray momentum by mirror scattering in the wave frame. The mirror force depends on the square of the perpendicular component of the velocity (Section 4.2), so TTD must operate with the pitch-angle scattering of gyroresonance to maintain momentum isotropy (Miller 1997).

A particle that interacts with an Alfvén wave can resonate only with the wavelength that is equal to the parallel gyrolength in the Doppler shifted frame, $(v_A - v_{\parallel}) 2\pi/\Omega$. A particle that interacts with magnetosonic waves can respond to the whole wave spectrum because it can choose the wave direction θ where the parallel wave speed equals its own (Schlickeiser & Miller 1998, Schlickeiser & Vainio 1999). In practice, such a wave field may not have the appropriate θ because wave damping is larger at higher θ .

TTD was originally thought to be such an important energy loss for the waves that the fast mode would not be important for cosmic rays (Schlickeiser 1994, Minter & Spangler 1997, Tsap 2000). Damping is large for high β because the thermal particles resonate with the waves and only highly parallel modes exist (Holman et al. 1979, Foote & Kulsrud 1979). However, $\beta \ll 1$ in the solar wind and in much of the cool dense phase of the ISM, and observations of the solar wind show that oblique and fast modes dominate over plane-parallel Alfvén waves (Tu, Marsch & Thieme 1989; Bieber, Wanner & Matthaeus 1996; Matthaeus, Goldstein & Roberts 1990). Thus, TTD particle acceleration could be important in parts of the ISM where β is small. The waves still have to be nearly isotropic to get effective scattering, though, and they should not be damped by other processes, such as ion-neutral or viscous friction. Such damping is important in most of the neutral medium where $\beta < 1$ is otherwise favorable for TTD (Kulsrud & Pearce 1969, Felice & Kulsrud 2001). This leaves few places where wave damping is low enough that TTD might be important.

Alfvén wave scattering is questionable too because of the extreme anisotropy of the fluctuations that may cascade down from pc scales to the gyroradius. Anisotropic turbulence produces tiny perpendicular irregularities that average out over a particle gyration (Chandran 2000a, 2001; Lerche & Schlickeiser 2001; Yan & Lazarian 2002; Teufel, Lerche & Schlickeiser 2003). The result is a scattering coefficient that is many orders of magnitude less than in the isotropic case. For this reason, Yan & Lazarian (2003a) reconsidered TTD scattering by fast modes at moderate β , emphasizing the isotropy of the fast waves and considering ISM regions where wave damping at particular cosmic ray energies is relatively small. The resolution of this damping problem for wave scattering is far from clear.

4.2. Other Scattering Mechanisms

The energy of fast cosmic ray gyrations is adiabatically invariant during slow changes in the magnetic field amplitude, so an increasing field puts more energy into the gyromotion while removing it from the parallel motion. This change, combined with momentum conservation, causes fast particles with high pitch angles to bounce off converging field lines. The mirror force is $-M\nabla_{\parallel}B$ for magnetic moment $M = mv_{\perp}^2/2B$ with particle mass m . This type of scattering involves very long wavelengths parallel to the field (Ragot 1999, 2000; Felice & Kulsrud 2001; Lu et al. 2002). The mirror sources could also be molecular clouds and clumps (Chandran 2000b).

Electric fields can also scatter cosmic rays. The flow of plasma at speed U transverse to a magnetic field generates an electric field, $\mathbf{E} = -\mathbf{U} \times \mathbf{B}$, that can be important in the parallel direction when the magnetic field has at least 2D structure, and it is convected around by turbulent motions (Fedorov et al. 1992, le Roux et al. 2002).

Transport transverse to the mean field occurs as individual field lines wander (Jokipii & Parker 1969, Bieber & Matthaeus 1997, Michalek & Ostrowski 1998, Giacalone & Jokipii 1999, Kóta & Jokipii 2000). This is important for radial diffusion in the solar wind, which has a spiral field (Chen & Bieber 1993), for diffusion in oblique shock fronts (Duffy et al. 1995), and for diffusion in the vertical direction out of the Galaxy. Magnetic fields with irregularities smaller than the gyroradius cause particles to skip over field lines, giving anomalous diffusion (Parker 1964; Chuvilgin & Ptuskin 1993; Casse, Lemoine & Pelletier 2002; Otsuka & Hada 2003; Erlykin et al. 2003). Braided field lines can lead to sub-diffusion (Getmantsev 1963), when the mean squared particle position in the cross field direction increases as the square root of time, instead of directly with time as in normal diffusion. Compound diffusion has both cross-field diffusion and diffusion along the field lines (Kirk et al. 1996). Cross diffusion requires a lot of perpendicular structure to the field lines over a diffusion length for the particle motion parallel to the field (Qin, Matthaeus & Bieber 2002). For ISM turbulence, the cross-field diffusion coefficient is 0.1–0.2 of the parallel coefficient (Chandran & Maron 2004a).

Shocks provide another site for cosmic ray scattering. Blandford & Ostriker (1980) considered an ISM made of cleared hot cavities from supernovae and showed how the resulting shocks could scatter and accelerate cosmic rays. Bykov & Toptygin (1985) extended this model to include secondary shocks that arise in the turbulence caused by the supernovae. Klepach, Ptuskin & Zirakashvili (2000) included stellar wind shocks. The composite spectrum of cosmic rays from an ensemble of shocks in a supersonically turbulent medium was determined by Schneider (1993). In such a medium, the summed energy distribution for cosmic rays from all of the shocks is close to a power law, but there can be flat parts or bumps, unlike the energy distribution from a single shock (see also Achterberg 1990, Bykov & Toptygin 1993).

4.3. Cosmic Ray Acceleration

Cosmic rays gain energy as they scatter off randomly moving parts of the ISM (Fermi 1949). This is momentum diffusion and called the second-order Fermi mecha-

nism because the energy gained per collision depends on the second power of the rms turbulent speed. It is reminiscent of the thermalization of a star cluster with the light particles gaining speed as they approach equilibrium with the heavy particles. Scott & Chevalier (1975) first applied this mechanism to supernova remnants, using random motions inside the remnant for scattering sites. Supernovae are a likely source for cosmic rays because the cosmic ray energy density, $\sim 1 \text{ eV cm}^{-3}$, divided by a $\sim 15 \text{ My}$ lifetime in the Galaxy, is about 5% of the total supernova power (Baade & Zwicky 1934, Ginzburg & Syrovatskii 1964).

Cosmic ray acceleration by momentum diffusion occurs throughout a compressibly turbulent ISM, not just in supernova remnants (Kulsrud & Ferrari 1978, Ptuskin 1988, Dolginov & Silant'ev 1990, Bykov & Toptygin 1993, Webb et al. 2003, Chandran & Maron 2004b). In a system of many shocks, particles that are trapped in the weak magnetic turbulence of the ambient medium also get accelerated every time these regions are compressed (Jokipii 1987).

Multiple shock crossings at the edge of a supernova remnant also accelerate cosmic rays (see review in Blandford & Eichler 1987). If the field is parallel to the shock direction, then magnetic turbulence created ahead of the shock by the outward streaming particles (Wentzel 1974, Skilling 1975) scatters these particles back into the shock where they encounter more turbulence. The post-shock turbulence was formerly pre-shock turbulence that got compressed and amplified (Schlickeiser, Campeanu & Lerche 1993; Vainio & Schlickeiser 1998). If the field is oblique to the shock direction, then gyromotions (Jokipii 1987) and field line wandering cycle particles through the front (Ragot 2001). Each time a particle cycles through the front it gains energy from the converging flow. This is called the first-order Fermi mechanism (Fermi 1954) because the energy gained per crossing depends on the first power of the shock velocity. About 10^{-3} of the incoming thermal particles are injected into cosmic rays (Pryadko & Petrosian 1997; Kang, Jones & Gieseler 2002; Bamba et al. 2003), with an efficiency depending on obliqueness (Ellison, Baring & Jones 1995; Kobayakawa, Honda, Samura 2002). Generally, the first-order mechanism dominates in strong shocks (Axford et al. 1977, Krymsky 1977, Bell 1978, Ostrowski 1994), although the second mechanism is more important downstream than upstream (Vainio & Schlickeiser 1998).

Shock acceleration explains the cosmic ray energy spectrum up to the “knee” at $\sim 10^{15} \text{ eV}$. The particles that stay in the shock longest end up with the most energy. The spectrum is a distribution function in the number of shock crossings, considering the continuous loss of particles that are trapped in the downstream flow (e.g., Kato & Takahara 2003).

Observations of the edge sharpness of supernova remnants suggest the amplitude of MHD waves near the shock is ~ 60 times the average ISM value (Achterberg, Blandford & Reynolds 1994). Simonetti (1992) observed a factor of at least 10 in the magnetic wave amplitude from Faraday rotation irregularities in a supernova remnant compared with the adjacent line of sight. The X-ray synchrotron emission from supernova remnants is direct evidence for acceleration of relativistic electrons (Koyama et al. 1995, Aschenbach & Leahy 1999).

4.4. Generation of Turbulence by Cosmic Rays

A collection of particles with a high enough density cannot stream along a magnetic field much faster than the Alfvén speed because they generate magnetic irregularities that scatter them (Lerche 1967; Wentzel 1968a, 1969; Kulsrud & Pearce 1969; Tadamaru 1969). The growth rate of the instability at wavenumber k for isotropic wave generation is (Cesarsky 1980)

$$\Gamma(k) \sim \Omega \left(\frac{n_{CR}(k)}{n_i} \right) \left(-1 + \frac{v_{stream}}{v_A} \right). \quad (8)$$

The first term in the parenthesis represents the stabilizing effect of wave damping from ion gyromotions. The second term drives the instability with a rate proportional to the ratio of the streaming speed to the Alfvén speed. The influence of collective effects is in the ratio of the density of those cosmic rays that resonate with wavenumber k to the background density of thermal ions. The size of the magnetic irregularity produced is about 2π times the particle gyroradius ($\sim 10^{13}$ cm for GeV energy and μ Gauss field), so more energetic particles make larger-scale field distortions. These distortions are not at the bottom of a turbulent cascade, so they should not be anisotropic (Chandran 2000a). They could cascade to give the ISM scintillation. The upper limit to the cosmic ray energy that can generate waves sufficient for their own scattering is around 100 to 1000 GeV (Cesarsky 1980, Yan & Lazarian 2003a). Much higher energies are possible in a Galactic wind model where the boundary between diffusion and advection depends on energy and the streaming instability Landau damps in a highly ionized Galactic halo (Ptuskin et al. 1997).

Hall (1980) suggested that waves generated by cosmic rays would damp quickly and proposed instead that scintillation-scale structures result from mirror and firehose instabilities in the hot ISM phase. Both require pressure anisotropies, which Hall notes should arise at the level of 0.01-0.1 if the hot medium is turbulent. The firehose instability requires $P_{\parallel} - P_{\perp} > B^2/4\pi$ for parallel and perpendicular pressures P_{\parallel} and P_{\perp} (Lerche 1966, Wentzel 1968b), and the mirror instability requires $P_{\perp} - P_{\parallel} > (B^2/4\pi) (P_{\parallel}/B_{\perp})$. These conditions are satisfied for anisotropy $|P_{\parallel} - P_{\perp}|/2P_{\parallel} \sim 0.01-0.1$ if the plasma $\beta = P/P_{mag}$ is very large, as might be the case in the hot intercloud medium if supernovae continuously sweep it free of gas and field.

5. RADIO WAVE SCINTILLATION AS A DIAGNOSTIC FOR ISM TURBULENCE

One of the earliest indications that the ISM is turbulent came from scintillation observations of electron density fluctuations on very small scales. These fluctuations cause diffraction and refraction of radio signals from pulsars and a few extragalactic sources. Diffraction broadens pulsar images, spreads out the pulse arrival times, and narrows the frequency interval over which the pulses have a coherent behavior. The relative motion of the diffracting medium also modulates the pulsar intensity on a timescale of minutes. Refraction from larger structures causes the images to split or wander in position and to vary in intensity on timescales of days to months. Scintillation effects like these offer many diagnostics for electron density structures

in the ionized interstellar medium, including *H II* regions, hot bubble edges and the ionized and hot intercloud media. Still, the origin of this turbulence is not clear. Because the scales are very small, typically 10^{15} cm or below, it could be part of a cascade from larger structures past the viscous length and down into the collisionless regime of MHD turbulence (section 4.11 in *Interstellar Turbulence I*), or it could be generated locally by cosmic ray streaming or other small-scale instabilities or by low-mass stellar winds and wakes (sections 3 and 4 in *Interstellar Turbulence I*). Here we review ISM scintillations. More extensive reviews may be found in Rickett (1977, 1990), Hewish (1992), and Cordes, Rickett & Backer (1988).

5.1. Theory of Diffraction and Refraction in the ISM

The index of refraction for radio waves is (Nicholson 1983)

$$\eta = 1 - 4\pi n_e r_e / k^2 \quad (9)$$

with electron density n_e , classical electron radius $r_e = e^2 / (m_e c^2) = 2.8 \times 10^{-13}$ cm, and wavenumber of the radio signal $k = 2\pi / \lambda$ for wavelength λ . The phase change of a signal that passes through a clump of size δx with an excess index of refraction $\delta\eta$ compared with a neighboring average region is $k\delta x\delta\eta$. The transmitted signal adds constructively to the neighboring signal at a relative propagation angle $\delta\theta$ if the difference in their path lengths, $\delta x \sin \delta\theta$, multiplied by k , equals the phase change. This gives $\delta\theta \sim \delta\eta = 4\pi\delta n_e r_e / k^2$ for small $\delta\theta$. This phase change is random for each clump the signal meets, so after $N = D / \delta x$ such clumps on a path length D , the root mean square angular change of the signal from diffraction is $\delta\theta_d = \delta\eta N^{1/2}$.

The most important clump size has a cumulative scattering angle $\delta\eta (D / \delta x)^{1/2}$ equal to the clump diffraction angle, $\delta\theta_d = (k\delta x)^{-1}$. Evaluation of $\delta\eta$ requires some knowledge of how δn_e depends on δx . For a turbulent medium, this relation comes from the power spectrum of electron density fluctuations,

$$P(\kappa) = C_n^2 \kappa^{-\alpha}, \quad (10)$$

where $\kappa = 1 / \delta x$ and $\alpha = 11/3$ for 3D turbulence with a Kolmogorov spectrum (we use κ here for the wavenumber of electron density fluctuations to distinguish it from the wavenumber k of the radio radiation used for the observation). The mean squared electron density fluctuation is obtained from the integral over phase space volume, $P(\kappa)4\pi\kappa^2 d\kappa$. For logarithmic intervals, this is approximately $\delta n_e^2 = P(\kappa)4\pi\kappa^3 \sim 4\pi C_n^2 \delta x^{\alpha-3}$. Thus, we have $\delta x \sim (16\pi\lambda^2 r_e^2 D C_n^2)^{-1/(\alpha-2)}$. Using the wave equation, Cordes, Pidwerbetsky & Lovelace (1986) got essentially the same result with $4\pi^2$ replacing 16π . The full theory more properly accounts for differences in the cumulative effects of the line-of-sight and transverse density variations. A recent modification considers power-law rather than Gaussian statistics for the clump size distribution (Boldyrev & Gwinn 2003).

For a reference set of parameters, e.g., GHz frequencies, kpc distances, and typical $C_n^2 \sim 10^{-4}$ meters $^{-20/3}$, the characteristic scale is $\delta x \sim 10^{10}$ cm. This small size implies that only pulsars and a few extragalactic radio sources can produce detectible

diffraction effects at radio frequencies. The smallness compared with the collisional mean free path of electrons also implies that the fluctuations have to be collisionless (see *Interstellar Turbulence I*).

Many observable properties of small radio sources give information, either directly or indirectly, about δx , which can be used to infer the strength and power index of the electron density fluctuation spectrum and its distribution on the line of sight. For example, the logarithm of the visibility of an interferometer is $-4\pi^2\lambda^2r_e^2s^{\alpha-2}SM$ where s is the baseline length and $SM = \int_0^D C_n^2 dz$ is the scattering measure. Spangler & Cordes (1998) found $\alpha \sim 3.65 \pm 0.08$ using this baseline dependence for 4 pulsars. Very long baseline interferometry (VLBI) observations of pulsar image sizes measure angular broadening as a function of frequency (Lee & Jokipii 1975a; Cordes, Pidwerbetsky & Lovelace 1986) and determine SM (Spangler et al. 1986). For the reference parameters, $\delta\theta_d \sim 0.15$ mas.

Angular broadening gives a spread in path lengths for the radio waves, and this corresponds to a spread in arrival times of pulses, $\tau = D\delta\theta_d^2/(2c)$ (Lee & Jokipii 1975b). Such pulse broadening scales as $\lambda^{2\alpha/(\alpha-2)}SM^{2/(\alpha-2)}D$, so the frequency dependence gives α and the absolute value gives SM for an assumed screen depth D . The flux density is correlated only over a small range of frequencies, $\delta\nu_d \sim (2\pi\tau)^{-1}$ (Salpeter 1969, Lee & Jokipii 1975b).

Pulsar amplitudes vary on a timescale $\delta t_d = \delta x/v_\perp \sim$ several minutes as a result of pulsar transverse motions $v_\perp \sim 100$ km s⁻¹ (Cordes 1986). Using the relations above, this can be rewritten $\delta t_d \sim (cD\delta\nu_d)^{1/2} / (2\pi^{1/2}\nu v_\perp)$. If pulsar distances and proper motions are also known, along with the dispersion measure, then the distribution of scattering material on the line of sight can be modeled (Harrison & Lyne 1993, Cordes & Rickett 1998).

Longer time variations (Sieber 1982) result from the changing refraction of radio signals in moving structures that have the diffraction angular size $\delta\theta_d$ or larger (Rickett, Coles & Bourgois 1984; Blandford & Narayan 1985). This angular size corresponds to a physical size for the refracting elements $\delta x_r = D\delta\theta_d$. For typical $\delta\theta_d \sim 0.1$ mas, $\delta x_r \sim 1.5 \times 10^{12}$ cm at $D = 1$ kpc. The corresponding refraction scintillation time is $\delta t_r = \delta x_r/v_\perp \sim$ days. Time variations over months are also observed from larger interstellar structures.

The relative rms amplitude of the source is the modulation index, $m = \langle (I - \langle I \rangle)^2 \rangle^{1/2} / \langle I \rangle$. For diffraction this can be 100%, but for refraction it is typically less than $\sim 30\%$ (Stinebring & Condon 1990, LaBrecque et al. 1994, Stinebring et al. 2000). The modulation index depends on the strength of scattering, which involves a length scale equal to the geometric mean of the scale for angular broadening and the dominant scale for electron density fluctuations, $(D\delta\theta_d\delta x)^{1/2}$. This is the Fresnel length, $r_F = (D/k)^{1/2}$, which is the transverse size of some object at distance D that is just small enough to show diffraction effects. When $r_F/\delta x_d$ is high, there are many diffracting elements of size δx_d inside each refracting element of size $D\delta\theta_d$, so diffraction is strong. For weak diffraction, the total phase change on the line of sight is small and the dominant clump size is the Fresnel length itself (Lovelace et al. 1970, Lee & Jokipii 1975c, Rickett 1990). In this case, the modulation index scales approximately with $(r_F/\delta x_d)^{\alpha-2} < 1$ (Lovelace et al. 1970). The modulation index measures

interstellar properties in this weak limit because then $m^2 \propto \lambda^{(\alpha+2)/2} D^{\alpha/2} C_n^2$, giving a diagnostic for C_n^2 and α (Rickett 1977). Small m usually corresponds to high frequencies, where diffraction is relatively unimportant.

Time variations can be visualized with a dynamic spectrum, which is a gray scale plot of intensity on a coordinate system of time versus frequency (Figure 2). Diffraction alone gives a random dynamic spectrum from the motion of unresolved objects of size δx , but larger refractive structures, which disperse their radio frequencies over larger angles, $\delta\theta \sim -2\theta\delta\nu/\nu$ (from the above expression $\delta\theta \sim 4\pi\delta n_e r_e/k^2$), sweep a spectrum of frequencies past the observer (Hewish 1980). The intensity peaks on a dynamic spectrum (averaged over many pulses) then appear as streaks with slope $dt/d\nu = -2D\delta\theta_d/(\nu v_\perp)$ (Cordes, Pidwerbetsky & Lovelace 1986); this can be used as a diagnostic for v_\perp . The right-hand part of Figure 2 is the 2D power spectrum of the dynamic spectrum. Stinebring et al. (2001) and Hill et al. (2003) suggest that the arcs arise from interference between a central image and a faint scattering halo 20–30 times larger.

Strong refraction can result in multiple images that produce interference fringes on a dynamic spectrum (Cordes & Wolszczan 1986; Rickett, Lyne & Gupta 1997). Multiple images imply that refraction, which determines the image separation, bends light more than diffraction, which determines the size. Because large-scale fluctuations dominate refraction, this observation implies either $\alpha > 4$, so that small wavenumbers dominate (Cordes, Pidwerbetsky & Lovelace 1986; Romani, Narayan & Blandford 1986), or there is additional structure on 10^{12} cm scales that is not part of a power law power spectrum (Rickett, Lyne & Gupta 1997).

5.2. Observations

Radio scintillation has been used to determine many properties of electron density fluctuations in the ISM. Diffraction and refraction come from the same electrons, so the ratio of their strengths is proportional to the ratio of the amplitudes of the electron density fluctuations on two different scales. From this ratio Armstrong, Rickett & Spangler (1995) derived the power spectrum of the fluctuations spanning > 6 orders of magnitude in scale. They determined $C_n^2 = 10^{-3} \text{ m}^{-20/3}$ and $\alpha = 11/3$ between 10^6 cm and 10^{13} cm. They also suggested from rotation measures ($\text{RM} = \int_0^D n_e B_{\parallel} dz$) that the same power law extends up to 10^{17} or 10^{18} cm.

Cordes, Weisberg & Boriakoff (1985) found $\alpha = 3.63 \pm 0.2$ using the relation between $\delta\nu_d$ and λ . They mapped the spatial distribution of C_n^2 from $\delta\nu_d$ observations of 31 pulsars, suggesting the Galaxy contains both thin and thick disk components. For the thin component, $C_n^2 \sim 10^{-3} - 1 \text{ m}^{-20/3}$ assuming $\alpha = 11/3$ and for the thick component, with $H > 0.5$ kpc, $C_n^2 \sim 10^{-3.5} \text{ m}^{-20/3}$. The rms level of electron density fluctuations at the dominant scale $\delta x \sim 10^{10}$ cm, which comes from the integral over the power spectrum (see above), was found to be $< \delta n_e^2 >^{1/2} \sim 5 \times 10^{-6} \text{ cm}^{-3}$ for the high latitude medium, for which $< n_e > \sim 0.03 \text{ cm}^{-3}$ from dispersion measures, and $< \delta n_e^2 >^{1/2} \sim 10^{-4.2} - 10^{-3.3} \text{ cm}^{-3}$ for the low latitudes.

Bhat, Gupta & Rao (1998) observed 20 pulsars for three years to average over

refraction variations and determined C_n^2 in the local ISM from $\delta\nu_d$. They observed an excess of scattering material at the edge of the local bubble, which also produced multiple images of one of these pulsars (Gupta, Bhat & Rao 1999). The edge of the local bubble may also have been seen by Rickett, Kedziora-Chudczer & Jauncey (2002) as a source of scattering in a quasar. Bhat & Gupta (2002) found a similar enhancement at the edge of Loop I, where $SM \sim 0.3 \text{ pc m}^{-20/3}$ and the density enhancement is a factor of ~ 100 over the surrounding gas. They also found excess scattering for more distant pulsars from the Sagittarius spiral arm.

Lazio & Cordes (1998a,b) used the angular sizes of radio sources and other information on lines of sight to the Galactic center and outer Galaxy to suggest that the scattering material is associated with the surfaces of molecular clouds. Ionized cloud edges were also suggested by Rickett, Lyne & Gupta (1997) to explain multiple images. Spangler & Cordes (1998) observed $\delta\theta_d$ from small sources behind six regions in the Cygnus OB1 association and found an excess in SM that was correlated with the emission measure, indicating again that scattering is associated with $H II$ regions. This result is consistent with the high cooling rate required by the dissipation of this turbulence, which implies high temperatures (Zweibel, Ferriere & Shull 1988; Spangler 1991; Minter & Spangler 1997).

The relation $v_\perp \sim (cD\delta\nu_d)^{1/2} / (2\pi^{1/2}\nu\delta t_d)$ combined with pulsar distances and proper motions led Gupta (1995) to determine a 1 kpc scale height for the scattering layer from long-term observations of 59 pulsars. Cordes & Rickett (1998) also used this method to find that scattering is rather uniformly distributed toward two pulsars, but for three lines of sight it was concentrated toward the pulsar, including Vela where the supernova remnant is known to contribute to the scattering (Desai et al. 1992); six other pulsars in that study had significant scattering from either a foreground spiral arm or $H II$ regions.

Bhat, Gupta & Rao (1999) compared $\delta\theta_d$ obtained from $\delta\nu_d$ with the angular size of the refraction pattern, $\delta\theta_r \sim (v_\perp/D)(dt/d\nu)$ from dynamic spectra. They showed that $\delta\theta_r/\delta\theta_d < 1$ for all 25 pulsars that had this data, implying that diffraction dominates refraction and therefore $\alpha < 4$. They also compared C_n^2 from $\delta\theta_r$ on the refractive scale with C_n^2 from $\delta\nu_d$ on the diffractive scale to determine the slope of the power spectrum directly (as did Armstrong et al. 1995). They found the Kolmogorov value $\alpha = 11/3$ to within the accuracy in most cases, but six pulsars, mostly nearby, gave slightly higher $\alpha \sim 3.8$. The longest-term variations had significantly more power than an extrapolation of the Kolmogorov spectrum, however, and the modulation indices were large, leading them to suggest an additional component of scattering electrons at scales of 10^{14} to 10^{15} cm. The same data led Bhat, Rao & Gupta (1999) to derive $\langle C_n^2 \rangle \sim 10^{-3.8} \text{ m}^{-20/3}$ and $\langle r_F/\delta x_d \rangle \sim 45$, indicating strong scattering.

Lambert & Rickett (2000) looked at the correlation between the modulation index for long-term variations from refraction and the relative decorrelation bandwidth, $\delta\nu_d/\nu$, which comes from diffraction. The correlation at 610 MHz for 28 sources fit Kolmogorov scaling ($\alpha = 11/3$) better than a shock-dominated model ($\alpha = 4$) model but at 100 MHz the Kolmogorov fit was not as good. They suggested that the minimum turbulent length was large, 10^{10} to 10^{12} cm instead of $< 10^9$ cm (Armstrong, Rickett & Spangler 1995). An excess of electron density structure at large scales could also explain the discrepancy.

Stinebring et al. (2000) monitored the modulation index of 21 pulsars for five years and found low values ($< 50\%$) that bracket $3.5 < \alpha < 3.7$ with no perceptible inner (smallest) scale for most of the pulsars. For the Crab, Vela, and four others, enhanced modulation indices were consistent with an inner scale of 10^{10} cm. Rickett, Lyne & Gupta (1997) suggested this excess scattering could be from AU-sized ionized clumps at cloud edges.

An inner scale of $5 \times 10^6 - 2 \times 10^7$ cm was found by Spangler & Gwinn (1990) after noting that interferometer baselines shorter than this had scintillation with $\alpha \sim 4$ whereas longer baselines had α near the Kolmogorov value, $-11/3$. They suggested the inner scale is caused by a lack of turbulence smaller than the ion gyroradius, v_{th}/Ω for thermal speed v_{th} , or by the ion inertial length, v_A/Ω , whichever is larger. This value of the inner scale is consistent with an origin of the scattering in the warm ionized medium or in $H II$ regions, but not in the hot coronal medium, which has much larger minimum lengths.

Shishov et al. (2003) studied pulsar PSR B0329+54 over a wide range of frequencies and found a power spectrum for electron density fluctuations with a slope of -3.5 ± 0.05 for lengths between 10^8 cm and 10^{11} cm. This spectrum is expected for turbulence in the Iroshnikov-Kraichnan model (see *Interstellar Turbulence I*). Shishov et al. noted how other lines of sight though the galaxy gave different spectra and suggested that the nature of the turbulence varies from place to place. They also found refraction effects on a scale of 3×10^{15} cm corresponding to electron density fluctuations of strength $\delta n_e \sim 10^{-2} \text{ cm}^{-3}$ and suggested these were neutral clouds with an overall filling factor of ~ 0.1 .

Scattering image anisotropy suggests anisotropic turbulence (see *Interstellar Turbulence I*). Lo et al. (1993) observed 2:1 anisotropy in images of Sgr A*, Wilkinson, Narayan & Spencer (1994) found scale-dependent anisotropic images of Cygnus X-3, Frail et al. (1994) observed 3:1 anisotropy in scattering of light from Galactic center OH/IR stars, whereas Trotter, Moran & Rodriguez (1998) observed axial ratios of 1.2–1.5 for quasar light that scatters through a local $H II$ region. A ratio of 4:1 was found for another quasar by Rickett, Kedziora-Chudczer & Jauncey (2002). Spangler & Cordes (1998) observed anisotropic scattering with axial ratio of 1.8 surrounding the Cygnus OB association and Desai & Fey (2001) observed axial ratios of ~ 1.3 toward the same region. The actual anisotropy of local fluctuations cannot be determined from these observations because many different orientations blend on the line of sight (Chandran & Backer 2002)

Extreme scattering events are observed in some extragalactic radio sources and a few pulsars. Their modulation is strong, $\geq 50\%$, they can last for several months, and they have light profiles that are flat-bottom with spikes at the end, or smooth bottom with no spikes (Fiedler et al. 1994). They may result from supernova shocks viewed edge-on (Romani, Blandford & Cordes 1987) or ionized cloud edges in the Galaxy halo (Walker & Wardle 1998). Some appear correlated with the edges of local radio loops (Fiedler et al. 1994, Lazio et al. 2000), in support of the shock model. The actual scattering process could be a combination of refractive defocusing, during which an intervening electron cloud produces a lens that diverges the light and makes the source dimmer (Romani et al. 1987, Clegg et al. 1998), or stochastic broadening by an excess of turbulence in a small cloud (Fiedler et al. 1987). Lazio et al. (2000) found an excess $SM = 10^{-2.5} \text{ kpc m}^{-20/3}$ associated with an event, corresponding to $C_n^2 \sim 10^7 \xi^{-1} (D/100 \text{ pc})^{-1} \text{ m}^{-20/3}$ for ratio ξ of the line-of-sight extent (D) to the

transverse extent. Fiedler et al. (1994) suggested $\langle \delta n_e^2 \rangle^{1/2} \sim 10^2/\xi \text{ cm}^{-3}$. This high level of scattering along with an observed increase in angular size during the brightness minimum (Lazio et al. 2000) suggests the scattering cloud is not part of a power spectrum of turbulence but is an additional AU-size feature (Lazio et al. 2000).

5.3. Summary of Scintillation

The amplitude, slope, and anisotropy of the power spectrum of interstellar electron density fluctuations have been observed by scintillation experiments. Estimates for the inner scale of these fluctuations range from 10^7 cm to 10^{10} cm or more. The shorter of these lengths is about the ion gyroradius in the warm ionized medium (Spangler & Gwinn 1990). This is much smaller than the mean free path for electron collisions so the fluctuations are collisionless (see *Interstellar Turbulence I*). A lower limit to the largest scale of $\sim 10^{18} \text{ cm}$ was inferred from rotation measures assuming a continuous power law for fluctuations, but this assumption is uncertain. The slope of the power spectrum is usually close to the Kolmogorov value, $-11/3$, and distinct from the slope for a field of discontinuities, which is -4 . Deviations from the Kolmogorov slope appear in some studies, and may be from a large inner scale, $\gg 10^9 \text{ cm}$, an excess of scattering sites having size $\sim 1\text{--}10 \text{ AU}$, or a transition in the scaling properties of the turbulence.

Scintillation arises from both the low-density, diffuse, ionized ISM and the higher-density *H II* regions, ionized cloud edges, and hot shells, where the amplitude of the power spectrum increases. On average, the relative fluctuations are extremely small, $\langle \delta n_e^2 \rangle^{1/2} / \langle n_e \rangle \sim 10^{-2}$ on scales that dominate the diffraction at GHz radio frequencies, $\delta x \sim 10^{10} \text{ cm}$ (Cordes et al. 1985). For a Kolmogorov spectrum, they would be larger on larger scales in proportion to $L^{2/3}$; if the spectrum is continuous up to pc scales, the absolute fluctuation amplitude there would be ~ 1 (Lee & Jokipii 1976). Anisotropy of scattered images is at the level of 50%, which is consistent with extremely large intrinsic anisotropies ($\times 1000$) from MHD turbulence (sections 4.11 and 4.13 in *Interstellar Turbulence I*) if many orientations on the line of sight are blended together.

6. Summary and Reflections

The turbulence that is observed directly on resolvable scales in the ISM also has important effects on very small scales, down to the level of atomic diffusion, mixing, and viscosity, and continuing far below to the thermal ion gyroradius. The resolvable turbulence in the neutral medium was reviewed in the first part of this series (*Interstellar Turbulence I*), along with general theory and simulations. The smaller scale implications were reviewed here.

Turbulence helps to disperse the elements made in supernovae and other stellar sources by stretching and folding the contaminated gas until the gradient length approaches the collision mean free path. Then atomic diffusion does the final step of interatomic mixing. This mixing and homogenization may occur partly at the

source, in the shock fronts and contact discontinuities around the expanding flow following dynamical instabilities, and it may occur partly in the ambient ISM after the expansion subsides.

Observations suggest that the dispersion in elemental abundances among stars inside clusters and field stars of the same age, and the abundance differences between HII regions and diffuse clouds, are only a few percent up to perhaps 30%. Observations of clusters also suggest that most of the mixing occurs within several times 10^8 years. This homogenization has to occur between the injection scale of supernovae and superbubble explosions and the star formation scale containing on the order of a solar mass. The corresponding range of spatial scales is ~ 100 for gas at the ambient density. Homogenization cannot be significant on scales much larger than a superbubble, because then it would diminish the galactic radial abundance gradient over a Hubble time. These gradients enter the problem in another way too because turbulence mixes the gas over galactic radius to increase the elemental dispersion locally at the same time as it mixes this gas locally and leads to homogenization.

While the distribution of elemental abundances appears to be fairly narrow, with a dispersion on the order of 10%, it may also have a fat tail caused by occasional odd stars and diffuse clouds with very different abundances. This tail is reminiscent of other fat tails in the distribution functions for turbulent media, and these other tails seem to originate with intermittency. In the case of elemental dispersion, this means that the homogenization process is spotty so some regions survive for long periods of time with very little mixing.

Several methods for studying turbulent mixing have been employed. Because of the wide range of scales involved, these studies often employ simplifying assumptions that appear to capture the essential physics. They include artificial stochastic velocity fields and closure methods using moment equations. Direct numerical simulations of ISM elemental dispersion have only just begun. The theory suggests that a turbulent medium mixes passive scalars like elemental abundances faster than a Gaussian velocity field because of the long-range correlations that are associated with turbulence.

Turbulence affects interstellar chemistry by mixing regions with different properties, heating the gas intermittently on the viscous scale, and enhancing ion-neutral collisions in regions with strong magnetic field gradients. Turbulent mixing is more far-reaching than diffusive mixing because of long-range correlated motions in a turbulent flow. Such mixing spreads out each chemical species over a large radial range inside a cloud. Turbulent heating promotes temperature-sensitive reactions inside otherwise cold clouds. Applications to the formation of CH^+ and OH in diffuse clouds look promising. Chemical reaction networks that include these turbulent processes are only beginning to understand some of the implications, and direct simulations of chemistry in a turbulent medium are limited to only a few studies so far.

The scattering and acceleration of cosmic rays depends strongly on the presence of turbulence in the ISM. The scale for this turbulence is the gyroradius, which is less than the collisional mean free path for most cosmic rays, which have energies less than 1 GeV. Thus, scattering relies entirely on magnetic irregularities in collisionless plasma turbulence. Cosmic ray acceleration is by two processes, both of which involve turbulence: The first-order Fermi mechanism accelerates cosmic rays by cycling them through shock fronts where they pick up a relative velocity kick comparable to the shock speed at each passage. This cycling occurs because magnetic irregularities on

each side of the front scatter the out-streaming cosmic rays back into the front. The second-order Fermi mechanism accelerates cosmic rays through turbulent diffusion. Each collision with a randomly moving magnetic irregularity turns the cosmic ray around with a reflection speed in the moving frame that is comparable to the incident speed. Over time, the result is a transfer of energy from the turbulence to the cosmic rays.

Cosmic ray scattering occurs in several ways. Fast moving particles can interact weakly but resonantly with numerous magnetic irregularities, and successive interactions of this type can randomly change the pitch angles of their helical motions along the field. This eventually leads to a complete reversal in the direction of motion. Cosmic rays can also interact strongly with large magnetic irregularities, as would occur in shock fronts and at the edges of dense cloud complexes. These interactions change the particle directions significantly each time. The nature of cosmic ray diffusion in both momentum and space is not understood well because the structure and strength of the important magnetic irregularities are not observed directly. If MHD turbulence is highly anisotropic on the scale of cosmic ray scattering, with transverse irregularities much stronger than parallel as suggested by theory, then resonant scattering processes during motions along the mean field can be very weak. The structure of magnetic waves below the mean free path is also unclear, as the usual fast and slow magnetosonic modes do not exist.

Cosmic rays can also generate turbulence by streaming instabilities following particle-wave resonances or by fire-hose and mirror instabilities that operate even without resonances. The expected anisotropy of Alfvén wave turbulence diminishes the first of these mechanisms significantly, however. The others are problematic because they require strong cosmic ray pressure anisotropies. As a result, the impact of cosmic rays on turbulence is currently not understood.

Radio wave scintillation is indirect evidence for interstellar plasma turbulence. These radio observations span a very wide range of spatial scales through a combination of diffraction and refraction effects. The scales are mostly below the collision mean free path, and they are far below the limits of angular resolution. The first of these limits makes it difficult to understand the origin of the density irregularities. Unlike the turbulence that scatters cosmic rays, which requires only magnetic irregularities and no density structure, the turbulence that causes scintillation requires small-scale density irregularities in the ionized medium. The associated magnetic irregularities are not observed, and the connection to cosmic ray scattering is unclear, even though the length scales are about the same. The origin of density structures below the collision mean free path is unknown. Atomic diffusion should smooth them out on a sound crossing time unless magnetic field irregularities hold them in place. In that case they could be the result of slight temperature variations, with the cooler regions having higher electron densities, all divided up and mixed together by transverse magnetic motions. The nature of these motions below the mean free path is unclear, because, as mentioned above, the usual fast and slow compressional modes do not exist, nor do the usual thermal and pressure-regulated processes.

The second of the two limits on spatial scale imply that the geometrical properties of scintillation turbulence are difficult to observe. The scintillation is clearly anisotropic, but whether it is in sheets or filaments, for example, is unknown.

The importance of scintillation observations for studies of ISM turbulence is that

they give the power spectrum of electron density fluctuations fairly accurately. This is usually close to the Kolmogorov spectrum of incompressible turbulence. Rarely are the spectra so steep that the medium can be interpreted as a superposition of sharp edges, like shock fronts. One recent observation with fairly high precision obtained the relatively shallow Iroshnikov-Kraichnan power spectrum, leading to the conjecture that the slope varies from region to region. As discussed in *Interstellar Turbulence I*, this variation may arise from a variation in the relative strength of the magnetic field compared to the turbulent motions, with the Iroshnikov-Kraichnan spectrum present in regions of relatively strong fields.

Observations suggest that scintillation arises in a distributed fashion from the ambient ionized medium and also from discrete high-density places like the edges of local bubbles, ionized molecular clouds, and HII regions. These discrete regions are likely to be highly turbulent and they also have a juxtaposition of hot and cool gas, which is necessary for isentropic mixing and electron density structure.

There are evidently many uncertainties in the nature of ISM turbulence on small scales, even though the evidence for this turbulence is pervasive. Part of the problem is that none of the features of this turbulence have been observed directly: not the densities, magnetic fields, temperatures, or motions. Still, the density irregularities are revealed indirectly through scintillation, the magnetic field irregularities through cosmic ray scattering, the temperature fluctuations through chemistry, and the motions through elemental and chemical mixing. An additional problem is that many small scale effects of ISM turbulence rely on details of the theory that are independent of the usual scaling relations, such as viscous heating and elemental diffusion, which arise at the bottom of the cascade in the neutral medium. Turbulence in the ionized medium is also below the collisional mean free path, where pressure and thermal effects are relatively unimportant. Moreover, the small scale ISM processes are often strongly dependent on the large scale processes, such as turbulent shock formation, energy and metal injection, and galactic-scale gradients. This means that direct simulations of small scale turbulence are impossible without simplifying assumptions about the large-scale medium – assumptions that require more knowledge about ISM turbulence on the large scale than is presently available.

While the observations and theory of ISM turbulence have come a long way from the first efforts in the 1950s, the details of this new information have led to a growing awareness that the complete problem is far too large to solve any time soon. We rely on future generations of astronomers and physicists to continue this work, and hope that they find this field as intriguing and challenging as we do today.

7. ACKNOWLEDGMENTS

We are grateful to A. Brandenburg, D. Lambert, F. Matteucci, S. Oey, and G. Tenorio-Tagle for helpful comments on Section 2; E. Falgarone, D. Hollenbach and J. Le Bourlot for helpful comments on Section 3; B. Chandran, R. Jokipii, A. Lazarian, V.S. Ptuskin, and R. Schlickeiser for helpful comments on Section 4; B. Rickett, S. Spangler, and D. Stinebring for helpful comments on Section 5 and to A. Hill for Figure 2.

REFERENCES

- Achterberg A. 1981. *Astron. Astrophys.* 98:161–72
- Achterberg A. 1990. *Astron. Astrophys.* 231:251–58
- Achterberg A, Blandford RD, Reynolds SP. 1994. *Astron. Astrophys.* 281:220–30
- Aguirre A, Hernquist L, Schaye J, Weinberg DH, Katz N, Gardner J. 2001. *Ap. J.* 560:599–605
- Andre MK, Oliveira CM, Howk JC, Ferlet R, Désert J-M, et al. 2003. *Ap. J.* 591:1000–12
- Andrievsky SM, Kovtyukh VV, Luck RE, Lépine JRD, Maciel WJ, Beletsky YuV. 2002. *Astron. Astrophys.* 392:491–99
- Argast D, Samland M, Gerhard OE, Thielemann F-K. 2000. *Astron. Astrophys.* 356:873–87
- Armstrong JW, Rickett BJ, Spangler SR. 1995. *Ap. J.* 443:209–21
- Aschenbach B, Leahy DA. 1999. *Astron. Astrophys.* 341:602–9
- Audouze J, Silk J. 1995. *Ap. J.* 451:L49–52
- Axford WI, Leer E, Skadron G. 1977. *Proc. Int. Cosmic Ray Conf., 15th, Plodiv, Bulgaria*, 11:132–37. Sofia: B'lgarska Akad. Naukite
- Baade W, Zwicky F. 1934. *Proc. Natl. Acad. Sci. USA* 20:259–63
- Balkovsky E, Falkovich G, Fouxon A. 2001. *Phys. Rev. Lett.* 86:2790–93
- Balsara D, Benjamin RA, Cox DP. 2001. *Ap. J.* 563:800–5
- Bamba A, Yamazaki R, Ueno M, Koyama K. 2003. *Ap. J.* 589:827–37
- Bateman NPT, Larson RB. 1993. *Ap. J.* 407:634–38
- Bec J, Gawedzki K, Horvai P. 2003. Intermittent distribution of tracers advected by a compressible random flow. (nlin.CD/0310015)
- Begelman MC, Fabian AC. 1990. *MNRAS* 244:P26–29
- Bell AR. 1978. *MNRAS* 182:147–56
- Berezinskii VS, Bulanov SV, Ginzburg VL, Dogiel VA, Ptuskin VS. 1990. *Astrophysics of Cosmic Rays*. Amsterdam: North Holland
- Bergin EA, Alves J, Huard T, Lada CJ. 2002. *Ap. J.* 570:L101–4
- Bettens RPA, Lee H-H, Herbst E. 1995. *Ap. J.* 443:664–74
- Bhat NDR, Gupta Y. 2002. *Ap. J.* 567:342–53

- Bhat NDR, Gupta Y, Rao AP. 1998. *Ap. J.* 500:262–79
- Bhat NDR, Gupta Y, Rao AP. 1999. *Ap. J.* 514:249–71
- Bhat NDR, Rao AP, Gupta Y. 1999. *Ap. J. Suppl.* 121:483–513
- Bieber JW, Matthaeus WH. 1997. *Ap. J.* 485:655–59
- Bieber JW, Wanner W, Matthaeus WH. 1996. *J. Geophys. Res.* 101:2511–22
- Black JH, van Dishoeck EF. 1991. In *Fragmentation of Molecular Clouds and Star Formation*, ed. E Falgarone, F Boulanger, G Duvert, pp. 139–50. Dordrecht: Kluwer
- Blackman EG, Field GB. 2002. *Phys. Rev. Lett.* 89:265007
- Blackman EG, Field GB. 2003. *Phys. Fluids.* 15:L73-6
- Blandford R, Eichler D. 1987. *Phys. Rep.* 154:1–75
- Blandford R, Narayan R. 1985. *MNRAS* 213:591–611
- Blandford RD, Ostriker JP. 1980. *Ap. J.* 237:793–808
- Boesgaard AM. 1989. *Ap. J.* 336:798–807
- Boffetta G, Celani A, Cristani A, Vulpiani A. 1999. *Phys. Rev. E* 60:6734–41
- Boffetta G, Sokolov IM. 2002. *Phys. Rev. Lett.* 88:094501
- Boland W, deJong T. 1982. *Ap. J.* 261:110–14
- Boldyrev S, Gwinn C. 2003. *Ap. J.* 584:791–96
- Bracco A, Chavanis PH, Provenzale A, Spiegel EA. 1999. *Phys. Fluids* 11:2280–87
- Brandenburg A, Kapyla P, Mohammed A. 2004. *Phys. Fluids* 16:1020-27
- Burke JR, Silk J. 1976. *Ap. J.* 210:341–64
- Bykov AM, Toptygin IN. 1985. *Sov. Astron. Lett.* 11:75–78
- Bykov AM, Toptygin IN. 1993. *Soviet Phys.-Uspekhi* 36:1020–1052
- Cameron AGW. 1973. *Icarus* 18:407–50
- Caputo F, Marconi M, Musella I, Pont F. 2001. *Astron. Astrophys.* 263:413–22
- Carraro G, Ng YK, Portinari L. 1998. *MNRAS* 296:1045–1056
- Cartledge SIB, Meyer DM, Lauroesch JT. 2003. *Ap. J.* 597:408–13
- Casse F, Lemoine M, Pelletier G. 2002. *Phys. Rev. D* 65:23002–16
- Cesarsky CJ. 1980. *Annu. Rev. Astron. Astrophys.* 18:289–319

- Chandran BDG. 2000a. *Phys. Rev. Lett.* 85:4656–59
- Chandran BDG. 2000b. *Ap. J.* 529:513–35
- Chandran BDG. 2001. *Space Sci. Rev.* 99:271–80
- Chandran BDG, Backer DC. 2002. *Ap. J.* 576:176–87
- Chandran BDG, Maron JL. 2004a. *Ap. J.* 602:170–80
- Chandran BDG, Maron JL. 2004b. *Ap. J.* 603:23–7
- Charnley SB. 1998. *MNRAS* 298:L25–28
- Charnley SB, Markwick AJ. 2003. *Astron. Astrophys.* 399:583–87
- Chen H, Chen S, Kraichnan RH. 1989. *Phys. Rev. Lett.* 63:2657–60
- Chen J, Bieber JW. 1993. *Ap. J.* 405:375–89
- Chen J-Y, Kollman W. 1994. See Libby & Williams 1994, pp. 211–308
- Chen YQ, Nissen PE, Zhao G, Zhang HW, Benoni T. 2000. *Astron. Astrophys. Suppl.* 141:491–506
- Chiappini C, Matteucci F, Romano D. 2001. *Ap. J.* 554:1044–1058
- Chuvilgin LG, Ptuskin VS. 1993. *Astron. Astrophys.* 279:278–97
- Clegg AW, Fey AL, Lazio TJW. 1998. *Ap. J.* 496:253–66
- Cordes JM. 1986. *Ap. J.* 311:183–96
- Cordes JM, Pidwerbetsky A, Lovelace RVE. 1986. *Ap. J.* 310:737–67
- Cordes JM, Rickett BJ. 1998. *Ap. J.* 507:846–60
- Cordes JM, Rickett BJ, Backer DC, eds. 1988. *Radio Wave Scattering in the Interstellar Medium, Am. Inst. Phys. Conf. Rep.* New York: Am. Inst. Phys.
- Cordes JM, Weisberg JM, Boriakoff V. 1985. *Ap. J.* 288:221–47
- Cordes JM, Wolszczan A. 1986. *Ap. J.* 307:L27–31
- Cunha K, Lambert DL. 1994. *Ap. J.* 426:170–91
- Cutler DJ, Groom DE. 1991. *Ap. J.* 376:322–34
- de Avillez MA, Mac Low M-M. 2002. *Ap. J.* 581:1047–1060
- Decamp N, Le Bourlot J. 2002. *Astron. Astrophys.* 389:1055–1067
- Deharveng L, Pena M, Caplan J, Costero R. 2000. *MNRAS* 311:329–45
- Desai KM, Fey AL. 2001. *Ap. J. Suppl.* 133:395–411

- Desai KM, Gwinn CR, Reynolds J, King EA, Jauncet D, et al. 1992. *Ap. J.* 393:L75–78
- Dolginov AZ, Silant'ev NA. 1990. *Astron. Astrophys.* 236:519–26
- Dopazo C. 1994. See Libby & Williams 1994, pp. 375–473
- Dopazo C, Valino L, Fueyo N. 1997. *Int. J. Mod. Phys. B* 11:2975–3014
- Doty SD, van Dishoeck EF, van der Tak FFS, Boonman AMS. 2002. *Astron. Astrophys.* 389:446–63
- Draine BT. 1985. In *Protostars and Planets II*, ed. DC Black, MS Matthews, pp. 621–40. Tucson: Univ. Ariz. Press
- Draine BT, Katz N. 1986. *Ap. J.* 310:392–407
- Dröge W. 1994. *Ap. J. Suppl.* 90:567–76
- Drury LO'C, Ellison DE, Aharonian FA, Berezhko E, Bykov A, et al. 2001. *Space Sci. Rev.* 99:329–52
- Duffy P, Kirk JG, Gallant YA, Dendy RO. 1995. *Astron. Astrophys.* 302:L21–24
- Edmunds MG. 1975. *Astrophys. Space Sci.* 32:483–91
- Edvardsson B, Andersen J, Gustafsson B, Lambert DL, Nissen PE, Tomkin J. 1993. *Astron. Astrophys.* 275:101–52
- Elitzur M, Watson WD. 1980. *Ap. J.* 236:172–81
- Elliott FW, Majda AJ. 1996. *Phys. Fluids* 8:1052–1060
- Ellison DC, Baring MG, Jones FC. 1995. *Ap. J.* 453:873–82
- Elmegreen BG. 1998. In *Abundance Profiles: Diagnostic Tools for Galaxy History*, ed. D Friedli, MG Edmunds, C Robert, L Drissen, ASP Conf. Ser., 147:278–86
- Engelmann JJ, Ferrando P, Soutoul A, Goret P, Juliusson E. 1990. *Astron. Astrophys.* 233:96–111
- Erlykin AD, Lagutin AA, Wolfendale AW. 2003. *Astrophys. Part.* 19:351–62
- Falgarone E, Puget JL. 1995. *Astron. Astrophys.* 293:840–52
- Falgarone E, Pineau des Forêts G, Roueff E. 1995. *Astron. Astrophys.* 300:870–80
- Falkovich G, Gawedzki K, Vergassola M. 2001. *Rev. Mod. Phys.* 73:913–76
- Fedorov YuI, Kats MF, Kichatinov LL, Stehlik M. 1992. *Astron. Astrophys.* 260:499–509
- Felice GM, Kulsrud RM. 2001. *Ap. J.* 553:198–210
- Feltzing S, Gonzalez G. 2001. *Astron. Astrophys.* 367:253–65

- Fermi E. 1949. *Phys. Rev.* 75:1169–74
- Fermi E. 1954. *Ap. J.* 119:1–6
- Ferrara A, Pettini M, Shchekinov Y. 2000. *MNRAS* 319:539–48
- Fessler JR, Kulick JD, Eaton JK. 1994. *Phys. Fluids* 6:3742–49
- Fiedler R, Dennison B, Johnston KJ, Waltman EB, Simon RS. 1994. *Ap. J.* 430:581–94
- Fiedler RL, Waltman EB, Spencer JH, Johnston KJ, Angerhofer PE, et al. 1987. *Ap. J. Suppl.* 65:319–84
- Fields BD, Turan JW, Cowan JJ. 2002. *Ap. J.* 575:845–54
- Fisk LA. 1976. *J. Geophys. Res.* 81:4633–50
- Flower DR, Pineau des Forêts G. 1998. *MNRAS* 297:1182–88
- Foote EA, Kulsrud RM. 1979. *Ap. J.* 233:302–16
- Fosalba P, Lazarian A, Prunet S, Tauber JA. 2002. *Ap. J.* 564:762–72
- Frail DA, Diamond PJ, Cordes JM, van Langevelde HJ. 1994. *Ap. J.* 427:L43–46
- Friel ED, Boesgaard AM. 1992. *Ap. J.* 387:170–80
- Frisch U. 1995. *Turbulence*. Cambridge: Cambridge Univ. Press. 296 pp.
- Fung JCH, Vassilicos JC. 1998. *Phys. Rev. E* 57:1677–90
- Garnett DR, Kobulnicky HA. 2000. *Ap. J.* 532:1192–96
- Gerola H, Glassgold AE. 1978. *Ap. J. Suppl.* 37:1–25
- Getmantsev GG. 1963. *Sov. Astron.* 6:477–79
- Giacalone J, Jokipii JR. 1999. *Ap. J.* 520:204–14
- Ginzburg V, Syrovatskii SI. 1964. *The Origin of Cosmic Rays*. Transl. HSH Massey, D ter Haar. New York: Macmillan
- Goldstein ML, Roberts DA, Matthaeus WH. 1995. *Annu. Rev. Astron. Astrophys.* 33:283–326
- Gredel R. 1997. *Astron. Astrophys.* 320:929–44
- Gredel R. 1999. *Astron. Astrophys.* 351:657–68
- Gredel R, Pineau des Forêts G, Federman SR. 2002. *Astron. Astrophys.* 389:993–1014
- Gupta Y. 1995. *Ap. J.* 451:717–23
- Gupta Y, Bhat NDR, Rao AP. 1999. *Ap. J.* 520:173–81

- Hall AN. 1980. *MNRAS* 190:353–69
- Hall DE, Sturrock PA. 1967. *Phys. Fluids* 10:2620–28
- Harrison PA, Lyne AG. 1993. *MNRAS* 265:778–80
- Hasselmann K, Wibberenz G. 1968. *Z. Geophys.* 34:353–88
- Heiles C. 1996. In *Polarimetry of the Interstellar Medium*, ed. WG Roberge, DCB Whittet, ASP Conf. Ser. 97:457–74. San Francisco: ASP
- Henry RRC, Worthey G. 1999. *PASP* 111:919–45
- Herbst E. 1999. In *Millimeter Wave Astronomy: Molecular Physics in Space*, ed. WF Wall, A Carramiñana, L Carrasco, pp. 341–54. Dordrecht: Kluwer
- Herr S, Wang L-P, Collins LR. 1996. *Phys. Fluids* 8:1588–1608
- Hewish A. 1980. *MNRAS* 192:799–804
- Hewish A. 1992. *Philos. Trans. R. Soc. London Ser. A* 341:167–76
- Higdon JC, Lingenfelter RE. 2003. *Ap. J.* 582:330–41
- Hill AS, Stinebring DR, Barnor HA, Berwick DE, Webber AB. 2003. *Ap. J.* 599:457–64
- Hollenbach D, McKee CF. 1989. *Ap. J.* 342:306–36
- Hollenbach DJ, McKee C. 1979. *Ap. J. Suppl.* 41:555–92
- Hollenbach DJ, Tielens AGGM. 1999. *Rev. Mod. Phys.* 71:173–230
- Holman GD, Ionson JA, Scott JS. 1979. *Ap. J.* 228:576–81
- Hou JL, Prantzos N, Boissier S. 2000. *Astron. Astrophys.* 362:921–36
- Howe JE, Ashby MLN, Bergin EA, Chin G, Erickson NR, et al. 2000. *Ap. J.* 539:L137–41
- Jokipii JR. 1966. *Ap. J.* 146:480–87
- Jokipii JR. 1987. *Ap. J.* 313:842–46
- Jokipii JR. 2001. *Astrophys. Space. Sci.* 277:15–26
- Jokipii JR, Parker EN. 1969. *Ap. J.* 155:777–98
- Jones FC, Lukasiak A, Ptuskin V, Webber W. 2001. *Ap. J.* 547:264–71
- Joulain K, Falgarone E, Pineau des Forêts G, Flower D. 1998. *Astron. Astrophys.* 340:241–56
- Jullien M-C, Castiglione P, Tabeling P. 2000. *Phys. Rev. Lett.* 85:3636–39
- Kang H, Jones TW, Gieseler UDJ. 2002. *Ap. J.* 579:337–58

- Kato TN, Takahara F. 2003. *MNRAS* 342:639–50
- Kaufman M. 1975. *Astrophys. Space. Sci.* 33:265–93
- Kennicutt RC Jr, Garnett DR. 1996. *Ap. J.* 456:504–18
- Kirk JG, Duffy P, Gallant YA. 1996. *Astron. Astrophys.* 314:1010–16
- Klepach EG, Ptuskin VS, Zirakashvili VN. 2000. *Astropart. Phys.* 13:161–72
- Klessen RS, Lin DN. 2003. *Phys. Rev. E* 67:046311
- Kobayakawa K, Honda YS, Samura T. 2002. *Phys. Rev. D* 66:083004
- Korpi MJ, Brandenburg A, Shukurov A, Tuominen I. 1999. *Astron. Astrophys.* 350:230–39
- Kóta J, Jokipii JR. 2000. *Ap. J.* 531:1067–1070
- Koyama K, Petre R, Gotthelf EV, Hwang U, Matsuura M, et al. 1995. *Nature* 378:255–58
- Kramer C, Alves J, Lada CJ, Lada EA, Sievers A, et al. 1999. *Astron. Astrophys.* 342:257–70
- Krymsky GF. 1977. *Dokl. Akad. Nauk SSSR* 243:1306–8
- Kulsrud R, Pearce WP. 1969. *Ap. J.* 156:445–70
- Kulsrud RM, Ferrari A. 1978. *Astrophys. Space Sci.* 12:302–18
- LaBrecque DR, Rankin JM, Cordes JM. 1994. *Astron. J.* 108:1854–59
- Lambert HC, Rickett BJ. 2000. *Ap. J.* 531:883–901
- Langer WD, van Dishoeck EF, Bergin EA, Blake GA, Tielens AGGM, et al. 2000. In *Protostars and Planets IV*, ed. VG Mannings, S Russell, pp. 29–58. Tucson: Univ. Ariz. Press
- Lazarian A, Vishniac ET. 1999. *Ap. J.* 517:700–18
- Lazio TJW, Cordes JM. 1998a. *Ap. J.* 505:715–31
- Lazio TJW, Cordes JM. 1998b. *Ap. J.* 497:238–52
- Lazio TJW, Fey AL, Dennison B, Mantovani F, Simonetti JH, et al. 2000. *Ap. J.* 534:706–17
- Lee LC, Jokipii JR. 1975a. *Ap. J.* 196:695–707
- Lee LC, Jokipii JR. 1975b. *Ap. J.* 201:532–43
- Lee LC, Jokipii JR. 1975c. *Ap. J.* 202:439–53
- Lee LC, Jokipii JR. 1976. *Ap. J.* 206:735–43

- Lee MA, Völk HJ. 1975. *Ap. J.* 198:485–92
- Lerche I. 1966. *Ap. J.* 145:806–10
- Lerche I. 1967. *Ap. J.* 147:689–96
- Lerche I, Schlickeiser R. 2001. *Astron. Astrophys.* 378:279–94
- le Roux JA, Zank GP, Milano LJ, Matthaeus WH. 2002. *Ap. J.* 567:155–58
- Lesieur M. 1990. *Turbulence in Fluids*. Dordrecht: Kluwer. 412 pp.
- Lewellen WS. 1977. In *Handbook of Turbulence*, ed. W Frost, TH Moulden, pp. 237–80. New York: Plenum
- Libby PA, Williams FA, eds. 1994. *Turbulent Reacting Flows*. New York: Academic. 474 pp.
- Lo KY, Backer DC, Kellermann KI, Reid M, Zhao JH, et al. 1993. *Nature* 362:38–40
- Lopez C, Puglisi A. 2003. *Phys. Rev. E.* 67:041302–5
- Lovelace RVE, Salpeter EE, Sharp LE, Harris DE. 1970. *Ap. J.* 159:1047–1055
- Lu JY, Zank GP, Rankin R, Marchand R. 2002. *Ap. J.* 576:574–86
- Lucas R, Liszt HS. 1997. In *Molecules in Astrophysics: Probes and Processes*, ed. EF van Dishoeck, IAU Symp. 178:421–30. Leiden: Kluwer
- Luck RE, Gieren WP, Andrievsky SM, Kovtyukh VV, Fouqué P, et al. 2003. *Astron. Astrophys.* 401:939–49
- Markiewicz WJ, Mizuno H, Völk HJ. 1991. *Astron. Astrophys.* 242:286–89
- Marscher AP, Moore EM, Bania TM. 1993. *Ap. J.* 419:L101–4
- Matthaeus WH, Goldstein ML, Roberts DA. 1990. *J. Geophys. Res.* 95:20673–83
- McComb WD. 1990. *Physics of Fluid Turbulence*. Oxford: Oxford Univ. Press. 572 pp.
- Meyer DM, Jura M, Cardelli JA. 1998. *Ap. J.* 493:222–29
- Michalek G, Ostrowski M. 1998. *Astron. Astrophys.* 337:558–64
- Miller JA. 1997. *Ap. J.* 491:939–51
- Minter AH, Spangler SR. 1997. *Ap. J.* 485:182–94
- Moore AP, Marscher AP. 1995. *Ap. J.* 452:671–79
- Moos HW, Sembach KR, Vidal-Madjar A, York DG, Friedman SD, et al. 2002. *Ap. J. Suppl.* 140:3–17
- Munakata K, Kiuchi T, Yasue S, Kato C, Mori S, et al. 1997. *Phys. Rev. D* 56:23–26

- Nejad LAM, Wagenblast R. 1999. *Astron. Astrophys.* 350:204–29
- Nicholson DR. 1983. *Introduction to Plasma Theory*. New York: Wiley
- Nicolleau F, Vassilicos JC. 2003. *Phys. Rev. Lett.* 90:024503
- O’Brien EE. 1980. In *Turbulent Reacting Flows*, ed. PA Libby, FA Williams, pp. 185–218. New York: Springer-Verlag
- Oey MS. 2000. *Ap. J.* 542:L25–28
- Oey MS. 2003. *MNRAS* 339:849–60
- Olszewski EW, Schommer RA, Suntzeff NB, Harris HC. 1991. *Astron. J.* 101:515–37
- Ostrowski M. 1994. *Astron. Astrophys.* 283:344–48
- Otsuka F, Hada T. 2003. *Space Sci. Rev.* 107:499–502
- Padoan P, Zweibel E, Nordlund A. 2000. *Ap. J.* 540:332–41
- Pan K, Federman SR, Welty DE. 2001. *Ap. J.* 558:L105–8
- Parker EN. 1964. *J. Geophys. Res.* 69:1755–58
- Paulson DB, Sneden C, Cochran WD. 2003. *Astron. J.* 125:3185–95
- Pavlovski G, Smith MD, Mac Low M-M, Rosen A. 2002. *MNRAS* 337:477–87
- Phillips TG, Huggins PJ. 1981. *Ap. J.* 251:533–40
- Pijpers FP. 1997. *Astron. Astrophys.* 325:300–4
- Piterbarg LI, Ostrovskii AG. 1997. *Advection and Diffusion in Random Media*. Dordrecht: Kluwer
- Pope SB. 1994. *Annu. Rev. Fluid Mech.* 26:23–63
- Pope SB. 2000. *Turbulent Flows*. Cambridge: Cambridge Univ. Press
- Prasad SS, Heere KR, Tarafdar SP. 1991. *Ap. J.* 373:123–36
- Prasad SS, Huntress WT. 1980. *Ap. J.* 239:151–65
- Pryadko JM, Petrosian V. 1997. *Ap. J.* 482:774–81
- Ptuskin VS. 1988. *Sov. Astron. Lett.* 14:255–57
- Ptuskin VS. 2001. *Space Sci. Rev.* 99:281–93
- Ptuskin VS, Soutoul A. 1998. *Astron. Astrophys.* 337:859–65
- Ptuskin VS, Völk HJ, Zirakashvili VN, Breitschwerdt D. 1997. *Astron. Astrophys.* 321:434–43
- Qin G, Matthaeus WH, Bieber JW. 2002. *Ap. J.* 578:L117–20

- Quillen AC. 2002. *Astron. J.* 124:400–3
- Ragot BR. 1998. *Ap. J.* 498:757–62
- Ragot BR. 1999. *Ap. J.* 518:974–84
- Ragot BR. 2000. *Ap. J.* 536:455–64
- Ragot BR. 2001. *Ap. J.* 547:1010–1023
- Rand RJ, Kulkarni SR. 1989. *Ap. J.* 343:760–72
- Reddy BE, Tomkin J, Lambert DL, Allende Prieto C. 2003. *MNRAS* 340:304–40
- Reeves H. 1972. *Astron. Astrophys.* 19:215–23
- Richardson LF. 1926. *Proc. R. Soc. London Ser. A* 110:709–37
- Rickett BJ. 1977. *Annu. Rev. Astron. Astrophys.* 15:479–504
- Rickett BJ. 1990. *Annu. Rev. Astron. Astrophys.* 28:561–605
- Rickett BJ, Coles WA, Bourgois G. 1984. *Astron. Astrophys.* 134:390–95
- Rickett BJ, Kedziora-Chudczer L, Jauncey DL. 2002. *Ap. J.* 581:103–26
- Rickett BJ, Lyne AG, Gupta Y. 1997. *MNRAS* 287:739–52
- Roberts H, Herbst E. 2002. *Astron. Astrophys.* 395:233–42
- Rocha-Pinto J, Maciel WJ, Scalo J, Flynn C. 2000. *Astron. Astrophys.* 358:850–68
- Rolleston WRJ, Dufton PL, Fitzsimmons A. 1994. *Astron. Astrophys.* 284:72–81
- Rolleston WRJ, Smartt SJ, Dufton PL, Ryans RSI. 2000. *Astron. Astrophys.* 363:537–54
- Rollinde E, Boisse P, Federman SR, Pan K. 2003. *Astron. Astrophys.* 401:215–26
- Romani RW, Blandford R, Cordes JM. 1987. *Nature* 328:324–26
- Romani RW, Narayan R, Blandford R. 1986. *MNRAS* 220:19–49
- Roy J-R, Kunth D. 1995. *Astron. Astrophys.* 294:432–42
- Salpeter EE. 1969. *Nature* 221:31–33
- Scalo JM. 1977. *Astron. Astrophys.* 55:253–60
- Schlickeiser R. 1989. *Ap. J.* 336:243–93
- Schlickeiser R. 1994. *Ap. J. Suppl.* 90:93629
- Schlickeiser R. 2002. *Cosmic Ray Astrophysics*. Berlin: Springer-Verlag. 519 pp.
- Schlickeiser R, Campeanu A, Lerche L. 1993. *Astron. Astrophys.* 276:614–24

- Schlickeiser R, Miller JA. 1998. *Ap. J.* 492:352–78
- Schlickeiser R, Vainio R. 1999. *Astrophys. Space Sci.* 264:457–69
- Schneider P. 1993. *Astron. Astrophys.* 278:315–27
- Scott JS, Chevalier RA. 1975. *Ap. J.* 197:L5–8
- Shematovich VI, Wiebe DS, Shustov BM, Li Z-Y. 2003. *Ap. J.* 588:894–909
- Shishov VI, Smirnova TV, Sieber W, Malofeev VM, Potapov VA, et al. 2003. *Astron. Astrophys.* 404:557–67
- Shraiman BI, Siggia ED. 2000. *Nature* 405:639–46
- Sieber W. 1982. *Astron. Astrophys.* 113:311–13
- Sigurgeirsson H, Stuart AM. 2002. *Phys. Fluids* 14:4352–61
- Silich SA, Tenorio-Tagle G, Terlevich R, Terlevich E, Netzer H. 2001. *MNRAS* 324:191–200
- Simonetti JM. 1992. *Ap. J.* 386:170–80
- Simpson JA, Garcia-Munoz M. 1988. *Space Sci. Rev.* 46:205–24
- Skilling J. 1975. *MNRAS* 173:245–54
- Slavin JD, Shull JM, Begelman MC. 1993. *Ap. J.* 407:83–99
- Spaans M. 1996. *Astron. Astrophys.* 307:271–87
- Spangler SR. 1991. *Ap. J.* 376:540–55
- Spangler SR, Cordes JM. 1998. *Ap. J.* 505:766–83
- Spangler SR, Gwinn CR. 1990. *Ap. J.* 353:L29–32
- Spangler SR, Mutel RL, Benson JM, Cordes JM. 1986. *Ap. J.* 301:312–19
- Stanimirovic S, Weisberg JM, Dickey JM, de la Fuente A, Devine K, et al. 2003. *Ap. J.* 592:953–63
- Stantcheva T, Herbst E. 2003. *MNRAS* 340:983–88
- Stinebring DR, Condon JJ. 1990. *Ap. J.* 352:207–21
- Stinebring DR, McLaughlin MA, Cordes JM, Becker KM, Goodman JEE, et al. 2001. *Ap. J.* 549:L97–100
- Stinebring DR, Smirnova TV, Hankins TH, Hovis JS, Kaspi VM, et al. 2000. *Ap. J.* 539:300–16
- Strong AW, Moskalenko IV. 1998. *Ap. J.* 509:212–28
- Tademaru E. 1969. *Ap. J.* 158:959–79

- Taillet R, Maurin D. 2003. *Astron. Astrophys.* 402:971–83
- Taylor GI. 1921. *Proc. London Math. Soc.* 20:196–202
- Tenorio-Tagle G. 1996. *Astron. J.* 111:1641–50
- Teufel A, Lerche I, Schlickeiser R. 2003. *Astron. Astrophys.* 397:777–88
- Thuan TX, Izotov YI, Lipovetsky VA. 1995. *Ap. J.* 445:108–23
- Tielens AGGM, Hollenbach D. 1985. *Ap. J.* 291:722–54
- Trotter AS, Moran JM, Rodriguez LF. 1998. *Ap. J.* 493:666–79
- Tsap YT. 2000. *Solar Phys.* 194:131–36
- Tu CY, Marsch E, Thieme KM. 1989. *J. Geophys. Res.* 94:11739–59
- Turner BE, Herbst E, Terzieva R. 2000. *Ap. J. Suppl.* 126:427–60
- Twarog BA, Ashman KM, Anthony-Twarog BA. 1997. *Astron. J.* 114:2556–85
- Vainio R, Schlickeiser R. 1998. *Astron. Astrophys.* 331:793–99
- van Dishoeck EF, Hogerheijde MR. 1999. In *The Origin of Stars and Planetary Systems*, ed. CJ Lada, ND Kylafis, pp. 97–140. Dordrecht: Kluwer
- Völk HJ, Jones FC, Morfill GE, Roser S. 1980. *Astron. Astrophys.* 85:316–25
- Walker M, Wardle M. 1998. *Ap. J.* 498:L125–28
- Warhaft Z. 2000. *Annu. Rev. Fluid. Mech.* 32:203–40
- Webb GM, Ko CM, Zank GP, Jokipii JR. 2003. *Ap. J.* 595:195–226
- Wentzel DG. 1968a. *Ap. J.* 152:987–96
- Wentzel DG. 1968b. *Ap. J.* 153:331–34
- Wentzel DG. 1969. *Ap. J.* 156:303–14
- Wentzel DG. 1974. *Annu. Rev. Astron. Astrophys.* 12:71–96
- Wielen R, Fuchs B, Dettbarn C. 1996. *Astron. Astrophys.* 314:438–47
- Wilkinson PN, Narayan R, Spencer RE. 1994. *MNRAS* 269:67–88
- Willacy K, Langer WD, Allen M. 2002. *Ap. J.* 573:L119–22
- Xie T, Allen M, Langer WD. 1995. *Ap. J.* 440:674–85
- Yan H, Lazarian A. 2002. *Phys. Rev. Lett.* 89:281102
- Yan H, Lazarian A. 2003a. Preprint
- Yan H, Lazarian A. 2003b. 592:L33-6

- Yanasak NE, Wiedenbeck ME, Mewaldt RA, Davis AJ, Cummings AC, et al. 2001. *Ap. J.* 563:768–92
- Yong D, Grundahl F, Lambert DL, Nissen PE, Shetrone MD. 2003. *Astron. Astrophys.* 402:985–1001
- Zweibel EG, Ferriere KM, Shull JM. 1988. In *Radio Wave Scattering in the Interstellar Medium. Am. Inst. Phys. Conf. Rep.*, pp. 70–73. New York: Am. Inst. Phys.

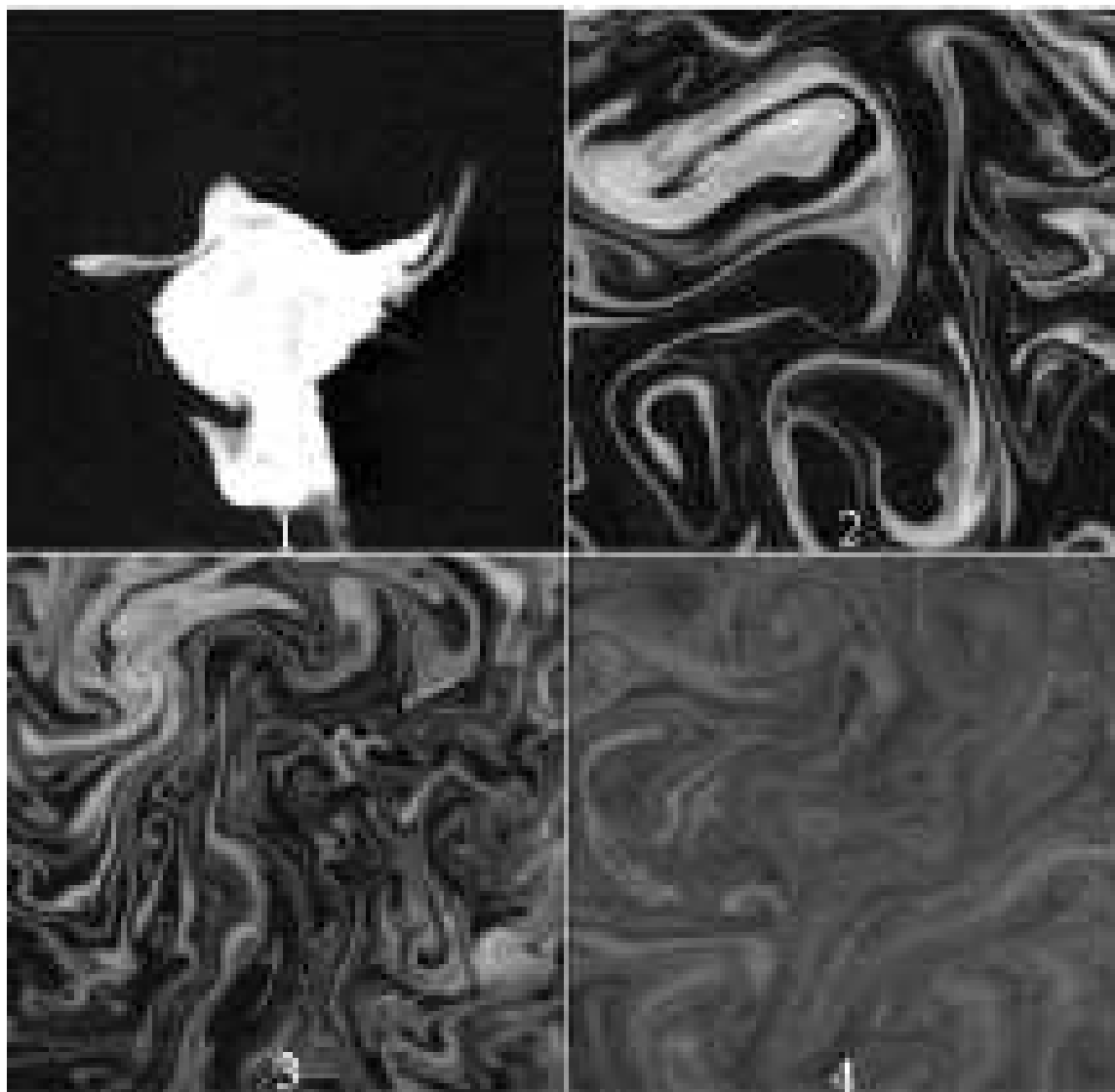


Fig. 1.— This sequence of four time steps shows a blob of dye released into an incompressible two-dimensional laboratory turbulent fluid that is forced by a chaotic velocity field with a single large scale. The evolution of this concentration field illustrates some of the basic features that can be expected for passive scalars like newly produced elements or dust grains released into the ISM: Nonlinear advection transports concentration away from the source but concentrates it locally through stretching and folding into thin regions of large velocity gradients where molecular diffusion eventually results in true mixing. From Jullien et al. (2000). *(for higher resolution, see paperII-f1.gif)*

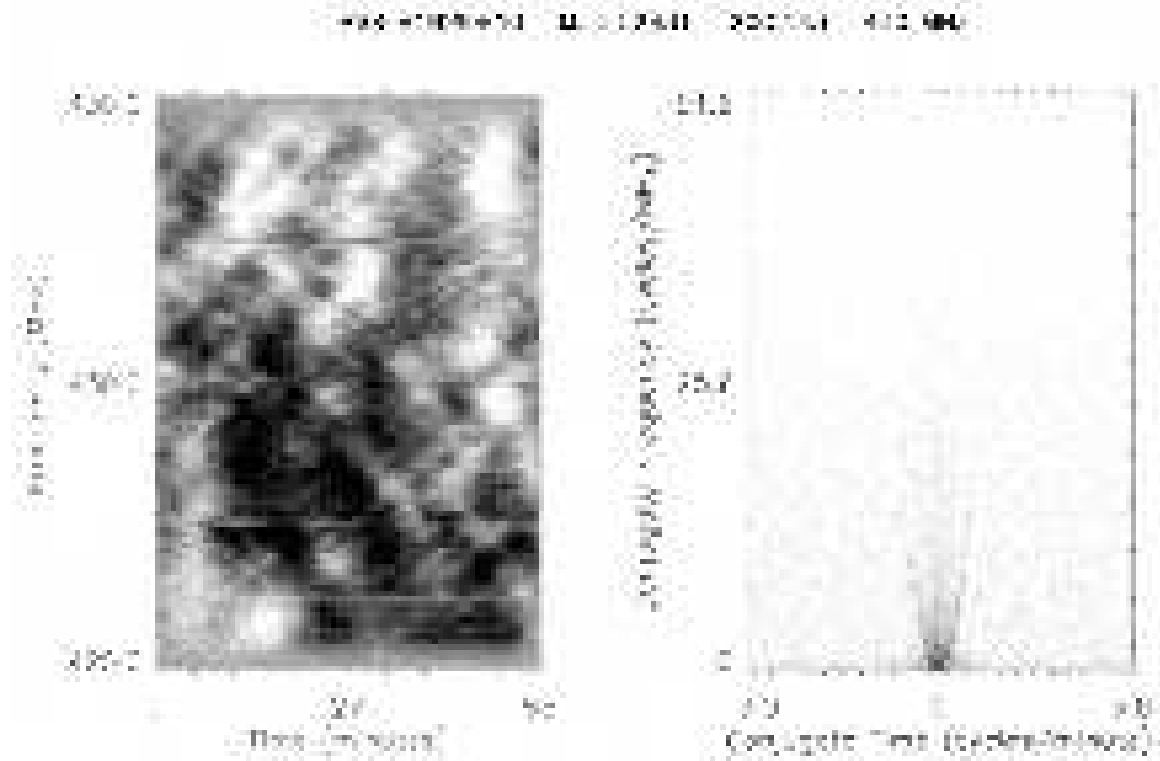


Fig. 2.— Dynamic spectrum of pulsar PSR B1929+10 (*left*) plotting flux density linearly with grayscale. The vertical columns are spectra, and many spectra are aligned horizontally in time. Intervening fluctuations in the electron density cause the signal to drift in both frequency and arrival time. A 2D Fourier transform of the dynamic spectrum is shown on the right. The crisscross pattern in the dynamic spectrum causes the parabolic boundary in the Fourier transform distribution. The grayscale for the secondary spectrum is logarithmic from 3 dB above the noise to 5 dB below the maximum (from Hill et al. 2003). (*for higher resolution, see paperII-f2.gif*)

This figure "paperII-f1.gif" is available in "gif" format from:

<http://arxiv.org/ps/astro-ph/0404452v1>

This figure "paperII-f2.gif" is available in "gif" format from:

<http://arxiv.org/ps/astro-ph/0404452v1>